



Department of Mathematical Sciences

Projection methods for Hamiltonian systems

Sindre Eskeland

February 16, 2016

MASTER thesis

Department of Mathematical Sciences

Norwegian University of Science and Technology

Supervisor: Professor Elena Celledoni

Preface

This is a master thesis as a part of the study program industrial mathematics. It was written during the winter 2015-2016.

Acknowledgment

Thanks to Elena Celledoni for guiding me, and Lu Li for giving me the theoretical insight this text needed. And trygve

Summary and Conclusions

To be filled in!

Contents

Preface	i
Acknowledgment	ii
Summary and Conclusions	iii
1 Introduction	2
2 TTD	4
3 Theory	5
3.1 Zero initial condition	5
3.2 Energy	6
3.3 Integration methods	6
3.3.1 Energy conservation for trapezoidal rule	7
3.4 Windowing	8
3.5 Solution methods	9
3.5.1 Arnoldi's Algorithm and the Krylov projection method	10
3.5.2 Symplectic Lanczos method	13
3.5.3 A comment on the orhogonalisation methods	18
3.5.4 Direct method	18
3.5.5 Linearity of the methods	19
3.5.6 Number of operations	21
3.6 SLM and its eigenvalue solving properties	21
4 Practice	24
4.1 Outdata	24

4.2 Pictures	25
4.3 Test problems	26
4.3.1 The wave equation	26
4.3.2 A random test problem	28
4.4 Implementation	29
5 Results for test problems with constant energy	30
5.1 Convergence	30
5.1.1 Numerical integration	31
5.1.2 Exact solvers	33
5.2 Convergence with the restart	33
5.2.1 convergence as a function of ι	34
5.3 Convergence with i_r	36
5.4 How to choose n	37
5.4.1 Without restart	37
5.4.2 With restart	38
5.4.3 For time domains	39
5.5 Energy and error	39
5.6 Residual energy	45
5.7 A different idea	45
5.7.1 Matlabs <code>expm</code> function	46
5.8 Computation time	47
5.8.1 Without restart	47
5.8.2 With restart	48
5.8.3 Windowing	49
5.8.4 With <code>expm</code>	50
6 Results for test problems with varying energy	51
6.1 Convergence	52
6.2 Convergence with ι	53
6.3 How to chose n	54

<i>CONTENTS</i>	1
6.4 Long time	54
6.5 Computation time	55
6.5.1 Without restart	56
6.5.2 With restart	56
7	58
7.1 Code	58
7.2 Further work	58
7.3 Conclusion	58

Chapter 1

Introduction

The equation

$$\begin{aligned}\dot{u}(t) &= Au(t) + p \cdot f(t) = g(t) \\ u(0) &= u_0\end{aligned}\tag{1.1}$$

often makes an appearance when solving partial differential equations with numerical methods. The author has earlier observed how the heat equation, discretized with finite difference methods to be on the form of equation (1.1) can be solved with the use of the Krylov projection method(KPM) [12], which uses Arnoldi's algorithm(Arnoldi) as orthogonalisation method. This note will continue on the same track, but with more focus on Hamiltonian discretizations of wave equations, random problems, and energy preservation. It will also feature a comparison between symplectic Lanczos method(SLM) [19] and Arnoldi. SLM is a projection technique that preserves the structure of Hamiltonian matrices. Due to this, SLM (claims to) preserve energy better than Arnoldi. This note will also compare time consumption and global error for the different methods.

There will also be a comparison between some different integration methods, and how the projection methods change when the time domain is divided into smaller pieces and each piece is considered independently with initial conditions from previous time domain.

Let the matrix I_j be the identity matrix with dimension j , and let

$$J_j = \begin{bmatrix} 0 & I_j \\ -I_j & 0 \end{bmatrix}. \tag{1.2}$$

A matrix A is said to be Hamiltonian if [22]

$$(JA)^\top = JA. \quad (1.3)$$

and symplectic if [13]

$$A^\top JA = J \quad (1.4)$$

!!!!!!!!!!!!!!Skrive litt mer her om hva som skal skje!!!!!!!!!!!!!!

Chapter 2

TTD

- Skrive bilde text, og fjerne labler fra bilder!
- Legg til hjelpe linjer på de plittene som trenger det, og kanskje ikke logg alle plottene som er det
- Skriv mer i introduksjonskap
- Det må overalt stå om ting er vektor eller skalar funksjon! (intro kap)
- send en 3 bilder til hAne
- Skal DM, KPM og SLM være texttt et??
- Løsningen på ligning 1 må skrives et sted (introduksjon)
- Skrive om applikasjoner i introduksjonen
- skrive at vi sammenligner med DM, som kanskje sluttet å fungere for lenge siden.
- Sjekk rekkefølgen på bildene!
- Skriv noe om grunnen til at jeg ikke sammneligner semirandom med expm løsning
- er SLM uten restart energi bevarende
- er SLM med restart energi bevarende
- Hvor raskt øker feilen for SLM med og uten restart.

Chapter 3

Theory

This chapter will contain the theoretical aspects of the projection methods, such as derivation, proof of convergence and assumptions.

3.1 Zero initial condition

For both KPM and SLM it is important that the initial conditions are zero. The reason for this is explained in section 3.5. Equation (1.1) can be transformed so that it has zero initial conditions in the following way [7]:

Start by shifting the solution

$$\hat{u}(t) = u(t) - u_0,$$

then rewrite the original equation as

$$\dot{\hat{u}}(t) = A\hat{u}(t) + Au_0 + pf(t)$$

$$\hat{u}(0) = 0.$$

The equation above solves the shifted problem, solve the original problem by shifting it back with

$$u(t) = \hat{u} + u_0.$$

All test problems with a non-zero initial condition will be transformed in this way without using the hat notation. The letter b will be used as a collective term to describe both Au_0 , or any

constant vector occurring on the right hand side of equation (1.1).

3.2 Energy

It is well known that the energy of a system on the form of equation (1.1) can be expressed as [10]

$$\mathcal{H}_1(u) = \frac{1}{2} u^\top(t) J A u(t) + u^\top(t) J p f(t) \quad (3.1)$$

If the transformation in section 3.1 is used, the energy is

$$\mathcal{H}_2(u) = \frac{1}{2} \hat{u}^\top(t) J A \hat{u}(t) + \hat{u}^\top(t) J(b + p f(t)). \quad (3.2)$$

For most theoretical derivation \mathcal{H}_2 will be used, as the shifted problem is the one actually solved. But in figures \mathcal{H}_1 is used since the unshifted problem is what is sought.

There will be a discussion about different types of test problem. The ones marked "constant energy" will be problems without a time dependent source term, meaning $f(t) = 0$. The other type is problems marked "varying energy", in this case $f(t)$ will be a non zero time dependent function. Test problems will be presented in section 4.3.

3.3 Integration methods

The time domain $[0, T_s]$ will be divided in k pieces, so that the step size is constant $h_t = 1/k$. The time discretized solution of $u(t_j)$ will be called U_j , with $t_j = j h_t$ where $j = 1, 2, \dots, k$, $j = 0$ is disregarded since the initial value is known to be zero. Let the discretization of $f(t_j)$ be called F_j . The integration methods considered in this text are trapezoidal rule, forward Euler, and midpoint rule. The definition and the iteration scheme of the different methods are given in table 3.1.

Trapezoidal rule and midpoint rule is the same method if the energy is constant. When F_j is not constant, midpoint rule should have an advantage because it is symplectic [?].

Trapezoidal rule [23]	$U_{i+1} = U_i + h_t g\left(\frac{1}{2}(t_i + t_{i+1}), \frac{1}{2}(U_i + U_{i+1})\right)$
	$U_{i+1} = (I - \frac{Ah_t}{2})^{-1} \left(U_i + \frac{h_t}{2} (AU_i + (F_{i+1} + F_i)) \right)$
Forward Euler [24]	$U_{i+1} = U_i + h_t g(t_i, U_i)$
	$U_{i+1} = U_i + h_t (AU_i + F_i)$
Midpoint rule [25]	$U_{i+1} = U_i + h_t g\left(t_{i+\frac{1}{2}}, \frac{1}{2}(U_i + U_{i+1})\right)$
	$U_{i+\frac{1}{2}} = U_i + \frac{h_t}{2} (AU_i + F_{\frac{1}{2}})$
	$U_{i+1} = (I - \frac{Ah_t}{2})^{-1} (U_{i+\frac{1}{2}} + \frac{h_t}{2} F_{i+\frac{1}{2}})$

Table 3.1: Methods for integrating in time. Note that since the midpoint rule uses the midpoint $F_{i+\frac{1}{2}}$, twice as many points needs to be saved for midpoint rule as for the other methods. Trapezoidal and midpoint rule have quadratic convergence rates, while forward Euler has linear convergence. To compare the methods it is therefore necessary to use the squared number of points for forward Euler as for the other methods.

Eigenvalue and diagonalization	$[V, D] = \text{eig}(A)$
	$U_i = V \cdot \text{diag}\left(\exp(\text{diag}(D \cdot t_i))\right) / V \cdot b - b$
Matlab's <code>expm</code> function	$U_i = \text{expm}(A \cdot t_i) \cdot b - b$

Table 3.2: Methods for exact integration in time. Since they are very computationally demanding they will only be used on small projected matrices. They also need the test problem to have constant energy. The expected convergence will be depending on the approximation of A , since this method is only exact in time. These function as explained in matlabs documentation: [1].

Forward Euler has no energy preserving properties, and is used to show the difference between a naive integration method, and energy preserving integration methods.

In addition to the iteration schemes in table 3.1 some exact solvers are used, they are presented in table 3.2.

3.3.1 Energy conservation for trapezoidal rule

This section will show the energy preserving properties of trapezoidal rule on the initial value shifted function

$$\begin{aligned} \dot{u}(t) &= Au + b \\ u(0) &= 0. \end{aligned} \tag{3.3}$$

Note that b can be any constant vector, not just Au_0 . The proof is based on [3]. The energy of this function has already been presented in equation (3.2). The main ingredients in this proof is the gradient of \mathcal{H}_1 , and the iterations scheme for the trapezoidal rule. Assume that A is a Hamiltonian matrix, so that JA is symmetric. The gradient of $\mathcal{H}_1(u)$ is

$$\nabla \mathcal{H}_1(u) = J(Au + b).$$

The trapezoidal rule found in table 3.1, used on equation (3.3) gives

$$\frac{U_{j+1} - U_j}{h_t} = A \frac{U_{j+1} + U_j}{2} + b.$$

Substituting $\frac{U_{j+1} + U_j}{2}$ for u gives the gradient of the energy of this function

$$\nabla \mathcal{H}_1\left(\frac{U_{j+1} + U_j}{2}\right) = JA \frac{U_{j+1} + U_j}{2} + Jb$$

Since $\frac{U_{j+1} - U_j}{h_t} = J^{-1} \nabla \mathcal{H}_1\left(\frac{U_{j+1} + U_j}{2}\right)$ and $\nabla \mathcal{H}_1\left(\frac{U_{j+1} + U_j}{2}\right)^\top J^{-1} \nabla \mathcal{H}_1\left(\frac{U_{j+1} + U_j}{2}\right) = 0$ we have

$$\nabla \mathcal{H}_1\left(\frac{U_{j+1} + U_j}{2}\right)^\top \frac{U_{j+1} - U_j}{h_t} = 0$$

Substituting $J(A \frac{U_{j+1} + U_j}{2} + b)$ for $\nabla \mathcal{H}_1\left(\frac{U_{j+1} + U_j}{2}\right)$, and solving the parenthesis gives

$$\mathcal{H}_1(U_{j+1}) - \mathcal{H}_1(U_j) = 0$$

So trapezoidal rule conserves the energy for functions with constant energy. Since the initial conditions are satisfied the energy will have the correct value at all times.

3.4 Windowing

As you will see, the projected methods has a tendency to stop working when the time domain is too large. A fix to this might be to divide the time domain in smaller pieces, and solve each piece individually. How this is done is described in the next paragraph.

Let T_s denote simulated time, let K be the number of pieces T_s is divided into, and let k be the number of pieces each K is divided into. Each of the K sub intervals is then solved as separate problems, with the initial conditions updated. This is explained in a more precise manner in algorithm 1. This method will be called "windowing", as this was the name my supervisor Elena Celledoni [2] used to describe the method.

Algorithm 1 Windowing

Start with an initial value U_0 , K and k .

Make an empty vector U .

for $j = 1, 2, \dots, K$ **do**

Solve differential equation with $k + 1$ points in time and initial value U_0 .

Place the new points at the end of U .

Update U_0 to be the last value of U .

Delete the last point of U .

end for

Return U .

3.5 Solution methods

There are two orthogonalisation methods that will be discussed in this text. Their names are symplectic Lanczos method(SLM), and Arnoldi's algorithm(KPM, as it is implemented as the Krylov projection method). The derivation of the methods, together with a proof of energy perseverance for SLM is presented in this section.

Projection methods are ways to make approximated solutions from a subset of the original problem by projecting a problem of several dimensions onto a smaller dimensional problem. One great feature of these methods is that a smaller system of equations can be used to obtain solutions, making further computations less demanding, but finding this projected system can be time consuming. An other drawback is that the projected solutions are approximations. The approximated solution can be improved by something called restarting, this means using the projection method again, to solve an equation for the difference between the projected solution, and the unprojected solution. This can be done repeatedly to obtain the desired accuracy.

Assume that the equations are on the form

$$\begin{aligned}\dot{u}(t) &= Au(t) + b \\ u(0) &= 0\end{aligned}\tag{3.4}$$

when these methods are used. Note that the initial values are zero as the restarts considers the difference between the projected solution and the unprojected solution, since it is difficult to know how well the initial value was approximated. It is also important that A is a Hamiltonian matrix when using SLM.

Note that the relation between \hat{m} , \tilde{n} , \tilde{m} used in the algorithms is given by $\hat{m} = 2\tilde{m} = 2(m-2)^2$ and $n = 2\tilde{n}$, where \hat{m} is the dimension of the system, and n is the size of the orthogonal system. n is sometimes called the restart variable. Don't worry too much about these details, it is just a way to simplify the expressions, the reason to simplify them this way will be described in section 4.3.

When talking about the true solution it is meant as the unprojected solution (the same problem, solved exactly the same way, except without any projection method), and will later be referred to as the direct method (DM).

3.5.1 Arnoldi's Algorithm and the Krylov projection method

This section is loosely based around the derivation of the method done in [8] and [12].

The Krylov subspace is the space $W_n(A, b) = \{b, Ab, \dots, A^{n-1}b\} = \{v_1, v_2, \dots, v_n\}$, where $n \leq \hat{m}$. The vectors v_i together with $h_{i,j} = v_i^\top A v_j$, are found by using Arnoldi's algorithm, shown in algorithm 2. Let V_n be the $\hat{m} \times n$ matrix consisting of column vectors $[v_1, v_2, \dots, v_n]$ and H_n be the $n \times n$ upper Hessenberg matrix containing all elements $(h_{i,j})_{i,j=1,\dots,n}$. Then the following holds [27]

$$\begin{aligned}
AV_n &= V_n H_n + h_{n+1,n} v_{n+1} e_n^\top \\
V_n^\top A V_n &= H_n \\
V_n^\top V_n &= I_n.
\end{aligned} \tag{3.5}$$

Algorithm 2 Arnoldi's algorithm[28]

Start with $A \in \mathbb{R}^{\hat{m} \times \hat{m}}$, $b \in \mathbb{R}^{\hat{m}}$, $n \in \mathbb{N}$ and a tolerance $\iota \in \mathbb{R}$.

$v_1 = b / \|b\|_2$

for $j = 1, 2, \dots, n$ **do**

 Compute $h_{i,j} = v_i^\top A v_j$, v_i for $i = 1, 2, \dots, j$

 Compute $w_j = Av_j - \sum_{i=1}^j h_{i,j} v_i$

$h_{j+1,j} = \|w_j\|_2$

if $h_{j+1,j} < \iota$ **then**

 STOP

end if

$v_{j+1} = w_j / h_{j+1,j}$

end for

Return H_n , V_n , v_{n+1} , $h_{n+1,n}$.

Here, e_n is the n th canonical vector in \mathbb{R}^n . n is the number of iterations performed with Arnoldi.

By using the transformation $u(t) \approx V_n z_n(t)$, equation (3.4) can, with the help of equation (3.5), be written as

$$\begin{aligned}
\dot{z}_n(t) &= H_n z_n(t) + \|b\|_2 e_1 f(t) \\
z_n(0) &= 0.
\end{aligned} \tag{3.6}$$

The approximated solution of the original problem can be attained by the following relation

$$u_n(t) = V_n z_n(t),$$

where u_n is the (approximated) solution found with n as a restart variable.

Convergence for the method can be shown by finding an expression for the residual, which

can be written as

$$r_n(t) = v f(t) - \dot{u}_n(t) + A u_n(t)$$

This can be rewritten with $u_n(t) = V_n z_n(t)$, to get

$$r_n(t) = v f(t) - V_n \dot{z}_n(t) + A V_n z_n(t)$$

By equation (3.5) it can be simplified to

$$r_n(t) = h_{n+1,n} e_n^\top z_n(t) v_{n+1} \quad (3.7)$$

Since $h_{n+1,n}$ is zero for some $n \leq \hat{m}$ (since $V_{\hat{m}} h_{n+1,n} v_{n+1} = 0$ by construction), the procedure will converge toward the correct solution $u(t)$.

Larger n gives better a approximation of the solution, but larger n also gives higher computational complexity. The drawback is also that there is no way of knowing how well the solution is approximated in advance, but the size of $h_{n+1,n}$ does say something about how well the solution is approximated(smaller $h_{n+1,n}$ means a smaller error), though it is only available after solving the problem. If the approximation is not sufficient the solution must be recalculated with larger n , unless you perform a restart.

A restart considers the difference $\epsilon_n^{(i)}(t) = u(t) - u_n^{(i)}$, as in equation (3.8). The iteration variable i is present since it is possible to restart several times, $u_n^{(i)}$ is the solution obtained after i restarts with n as a restart variable.

$$\dot{\epsilon}_n^{(i)}(t) = A \epsilon_n^{(i)}(t) - r_n^{(i)}. \quad (3.8)$$

Where

$$r_n^{(i)} = h_{n+1,n}^{(i-1)} v_{n+1}^{(i-1)} e_n^\top \epsilon_n^{(i-1)}(t), \quad (3.9)$$

which is exactly the same as in equation (3.7), except that $z_n(t)$ is replaced with $\epsilon_n(t)$, and the counter i is present. Equation (3.8) can be simplified by using equation (3.5), and writing

$\epsilon_n^{(i)}(t) = V_n \delta_n^{(i)}(t)$, to obtain equation (3.10).

$$\dot{\delta}_n^{(i)}(t) = H_n^{(i)} \delta_n^{(i)}(t) + e_1 h_{n+1,n}^{(i-1)} e_n^\top \delta_n^{(i-1)}(t), \quad i \geq 1 \quad (3.10)$$

The solution is found by $u_n^{(i)}(t) = \sum_{j=0}^i S_n^{(j)} \delta_n^{(j)}(t)$, where $\delta_n^{(0)}(t) = z_n(t)$ and found by equation (3.6). H_n , v_{n+1} , $h_{n+1,n}$ and V_n without counting variables will also be referring to equation (3.6).

Repeatedly solving this equation can increase the accuracy of the approximated solution within an arbitrary constant of the desired solution. It is no longer possible to use $h_{n+1,n}$ as a measure for the error when the restart is used, since Arnoldi's algorithm has no way to measure how much this iteration improved the solution compared to previous iterations.

The proof for the convergence of the restart can be found in [9].

3.5.2 Symplectic Lanczos method

SLM and KPM are very similar, which is easy to see when comparing equation (3.5) and (3.11). The main difference is that orthonormality in Arnoldi is replaced by symplecticity in SLM. This makes the derivation quite similar.

Let $S_n = [v_1, v_2, \dots, v_{\frac{n}{2}}, w_1, w_2, \dots, w_{\frac{n}{2}}]$ be a set of J -orthogonal vectors satisfying the following equations [14]

$$\begin{aligned} AS_n &= S_n H_n + \zeta_{n+1} v_{n+1} e_{\hat{m}}^\top \\ J_n^{-1} S_n^\top J_{\hat{m}} A S_n &= H_n \\ S_n^\top J_{\hat{m}} S_n &= J_n \end{aligned} \quad (3.11)$$

Here S_n is an $\hat{m} \times n$ matrix, H_n is an $n \times n$ matrix, where $\tilde{n} = \frac{n}{2}$ is the number of iterations the algorithm performed, this is because the algorithm makes two vectors per iterations: v_j and w_j .

Algorithm 3 Symplectic Lanczos method [19], with reorthogonalization from [18].

Start with a Hamiltonian matrix $A \in \mathbb{R}^{2\tilde{m} \times 2\tilde{m}}$, $b \in \mathbb{R}^{2\tilde{m}}$, $\tilde{n} \in \mathbb{N}$

$$v_0 = 0 \in \mathbb{R}^{2\tilde{m}}$$

$$\zeta_1 = \|b\|_2$$

$$v_1 = \frac{1}{\zeta_1} b$$

for $j = 1, 2, \dots, \tilde{n}$ **do**

$$v = Av_j$$

$$\delta_j = v_j^\top v$$

$$\tilde{w} = v - \delta_j v_j$$

$$\kappa_j = v_j^\top J_{\tilde{m}} v$$

$$w_j = \frac{1}{\kappa_j} \tilde{w}_j$$

$$w = Aw^j$$

$$\tilde{S}_{j-1} = [v_1, v_2, \dots, v_{j-1}, w_1, w_2, \dots, w_{j-1}]$$

$$w_j = w_j + \tilde{S}_{j-1} J_{j-1} \tilde{S}_{j-1}^\top J_{\tilde{m}} w_j$$

$$\beta = -w_j^\top J_{\tilde{m}} w$$

$$\tilde{v}_{j+1} = w - \zeta_j v_{j-1} - \beta_j v_j + \delta_j v_j$$

$$\zeta_{j+1} = \|\tilde{v}_{j+1}\|_2$$

$$v_{j+1} = \frac{1}{\zeta_{j+1}} \tilde{v}_{j+1}$$

$$\tilde{S}_j = [v_1, v_2, \dots, v_j, w_1, w_2, \dots, w_j]$$

$$v_{j+1} = v_{j+1} + \tilde{S}_j J_j \tilde{S}_j^\top J_{\tilde{m}} v_{j+1}$$

end for

$$S_n = [v_1, v_2, \dots, v_{\tilde{n}}, w_1, w_2, \dots, w_{\tilde{n}}]$$

$$H_n = \begin{bmatrix} \text{diag}([\delta_j]_{j=1}^{\tilde{n}}) & \text{tridiag}([\zeta_j]_{j=2}^{\tilde{n}}, [\beta_j]_{j=1}^{\tilde{n}}, [\zeta_j]_{j=2}^{\tilde{n}}) \\ \text{diag}([\kappa_j]_{j=1}^{\tilde{n}}) & \text{diag}([- \delta_j]_{j=1}^{\tilde{n}}) \end{bmatrix}$$

Return H_n , S_n , v_{n+1} , ζ_{n+1} .

The process of making the vectors and matrix is a little more involved than for Arnoldi's algorithm, so there will be no thorough explanation of how it works, except for in Algorithm 3.

Transform the problem in equation (3.4) with $u(t) \approx S_n z_n(t)$, multiply with $J_n^{-1} S_n^\top J_{\hat{m}}$, and simplify with equation (3.11) to obtain

$$\dot{z}(t) = H_n z_n(t) + J_n^{-1} S_n^\top J_{\hat{m}} b f(t).$$

This can be further simplified when writing $b = S_n e_1 \|b\|_2$ and using equation (3.11):

$$\dot{z}(t) = H_n z_n(t) + \|b\|_2 e_1 f(t). \quad (3.12)$$

Equation (3.12) and (3.6) are identical, except for the orthogonalization method used.

Since $S_{\hat{m}}^\top J_{\hat{m}} \zeta_{n+1} v_{n+1} = 0$ by construction [20], the proof of convergence will be very similar to the proof for KPM.

The residual of the method can be written as

$$r_n(t) = v f(t) - \dot{u}_n(t) A u_n(t). \quad (3.13)$$

This can be rewritten with $u_n = S_n z_n(t)$.

$$r_n(t) = v f(t) - S_n \dot{z}_n(t) + A S_n z_n(t). \quad (3.14)$$

By equation (3.11) it becomes

$$r_n(t) = \zeta_{n+1} v_{n+1} e_{\hat{m}}^\top z(t). \quad (3.15)$$

Since ζ_{n+1} will approach zero as n grows, r_n will approach zero, and the method will converge.

A restart can also here be performed if the accuracy of the solution is not satisfactory. This

can be derived by looking at the difference $\epsilon_n = u(t) - S_n z_n(t)$:

$$\dot{\epsilon}_n^{(i)}(t) = A\epsilon_n^{(i)}(t) + r_n^{(i)}(t), \quad (3.16)$$

where

$$r_n^{(i)}(t) = \zeta_{n+1}^{(i-1)} v_{n+1}^{(i-1)} e_{\hat{m}}^\top \epsilon_n^{(i-1)}(t).$$

Write $\epsilon_n^{(i)}(t) = V_n \delta_n^{(i)}(t)$ to obtain

$$\dot{\delta}_n^{(i)} = H_n^{(i)} \delta_n^{(i)} + J_n^{-1} S_n^{(i)\top} J_{\hat{m}} \zeta_{n+1}^{(i-1)} v_{n+1}^{(i-1)} e_n^\top \delta_n^{(i-1)}.$$

This can be further simplified to

$$\dot{\delta}_n^{(i)} = H_n^{(i)} \delta_n^{(i)} + e_1 \zeta_{n+1}^{(i-1)} e_n^\top \delta_n^{(i-1)}, \quad i \geq 1. \quad (3.17)$$

The solution is found by $u_n^{(i)}(t) = \sum_{j=0}^i S_n^{(j)} \delta_n^{(j)}(t)$, where $\delta_n^{(0)}(t) = z_n(t)$ and found by equation (3.12). H_n , v_{n+1} , ζ_{n+1} and S_n without counting variables will also be referring to equation (3.12)

Proof of convergence and other interesting results for this method can be found in [21].

Proof that SLM without restart is energy preserving

If equation (3.12) is solved by an energy preserving method, eg. trapezoidal rule, the energy will be preserved [11]. The energy of this equation is

$$\mathcal{H}(z_n) = \frac{1}{2} z_n(t)^\top J_n H_n z_n(t) + z_n(t)^\top J_n e_1 \|b\|_2$$

While the energy of the original problem is

$$\mathcal{H}(u_n) = \frac{1}{2} u_n(t)^\top J A u_n(t) + u_n(t)^\top J b.$$

Perform the substitution $u_n(t) = S_n z_n(t)$ and get

$$\mathcal{H}(u_n) = \frac{1}{2} z_n(t)^\top S_n^\top J A S_n z_n(t) + z_n(t)^\top S_n^\top J b$$

use that $b = S_n e_1 \|b\|_2$, and simplify with equation (3.11).

$$\mathcal{H}(u_n) = \frac{1}{2} z_n(t)^\top J_n H_n z_n(t) + z_n(t)^\top J_n e_1 \|b\|_2$$

And we see that

$$\mathcal{H}(z_n) - \mathcal{H}(u_n) = 0$$

So the transformation does not change the energy, thus SLM is energy preserving. This will not hold for KPM for a couple of reasons. First H_n is not a Hamiltonian matrix, so the method it self is not energy preserving. The other reason is that the transformation V_n is not symplectic. SLM with restart is also not energy preserving since the error equation is depending on time, which ruins the energy preserving properties. But this property can be somewhat regain by restarting several times.

Residual energy

Equation (3.18) and (3.19) are solemnly used to describe the residual energy of the methods. \mathcal{H}_3 describes the residual energy of the projected method, in u_n space, that is, after transforming back from z_n space. \mathcal{H}_4 is the residual energy in z_n space. In theory these energies should be equal and zero. Section 5.6 shows how this holds up in practice. They are presented in the equation below, and can easily be derived from (3.16) and (3.17).

$$\mathcal{H}_3(t) = \frac{1}{2} \epsilon^{(1)\top}(t) J_m A \epsilon^{(1)} + \epsilon^{(1)\top} J_m h_{n+1,n}^{(1)} v_{n+1}^{(1)} e_n^\top z(t) \quad (3.18)$$

$$\mathcal{H}(t) = \frac{1}{2} \delta^{(1)\top}(t) J_n H_n^{(2)} \delta^{(1)} + \delta^{(1)\top} S_n^{(2)\top} J_m h_{n+1,n}^{(1)} v_{n+1}^{(1)} e_n^\top z(t) \quad (3.19)$$

The iteration variables are present since it considers the residual with one restart.

3.5.3 A comment on the orthogonalisation methods

The derivation of the methods above shows the vast similarities between SLM and KPM. The only practical difference between the two methods are the orthogonalisation methods. This makes implementation of the methods very similar.

How to obtain the correct number of restarts to get a good estimate of the solution will be discussed in section 4.4 and 5.4.

3.5.4 Direct method

It is important to have some method to compare with these projection methods with. This will be done by solving the problem exactly the same way, but without using any projection method, this will be called direct method, or DM.

The energy of DM will be constant if an energy preserving method is used, while the error will increase linearly [?]. A goal of this text is to see how KPM and SLM's error and energy behaves compared to this.

The proof that DM is the natural method to compare with will be shown here with trapezoidal rule for KPM. The proof is very similar for SLM.

We start by stating the desired equation discretized with the trapezoidal rule:

$$(I - \frac{Ah_t}{2})U_{i+1} = \left(U_i + \frac{h_t}{2}(AU_i + F_{i+1} + F_i) \right).$$

Applying the transformation $U_i = V_n Z_i(t)$ gives

$$(V_n - \frac{AV_n h_t}{2})Z_{i+1} = \left(V_n Z_i + \frac{h_t}{2}(AV_n Z_i + F_{i+1} + F_i) \right).$$

Using equation (3.5) gives

$$\left(V_n - h_t \frac{V_n H_n + h_{n+1,n} v_{n+1} e_n^\top}{2} \right) Z_{i+1} = \left(V_n Z_i + \frac{h_t}{2} ((V_n H_n + h_{n+1,n} v_{n+1} e_n^\top) Z_i + F_{i+1} + F_i) \right).$$

When using the trapezoidal rule directly on (3.6), the result is

$$\left(V_n - h_t \frac{V_n H_n}{2} \right) Z_{i+1} = \left(V_n Z_i + \frac{h_t}{2} (V_n H_n Z_i + F_{i+1} + F_i) \right).$$

If we now let n grow, $h_{n+1,n}$ will become zero and the projected method will converge towards the unprojected method.

3.5.5 Linearity of the methods

The projection methods require a vector that can be used to generate the orthogonal space. In the general problem,

$$\dot{u}(t) = Au(t) + b, \quad (3.20)$$

b is used to create the orthogonal space. But what if instead of just b , there were some time dependence, eg. $b + F(t)$, or (more illustrative)

$$\dot{u}(t) = Au(t) + b + F(t) \quad (3.21)$$

In this case the projection method needs to be used two times, one time to solve $\dot{u}(t) = Au + b$ and another to solve $\dot{u}(t) = Au + F(t)$. The solutions can then be added together to solve the original problem.

The reason for this is the need for a vector that can generate the orthogonal space. In this case there is no common vector \tilde{b} so that $\tilde{b}\tilde{F}(t) = b + F(t)$.

An even bigger problem arises when a differential equation has a source term that is not separable in time and space, read more about the reason for this in [8] and [12]. An equation that is separable in time and space can be written as $p(t, x, y) = g(x, y) \cdot F(t)$. If $p(t, x, y)$ is not separable, this is impossible. As an example, consider the wave equation

$$\frac{\partial^2 q(t, x, y)}{\partial t^2} = \frac{\partial^2 q(t, x, y)}{\partial x^2} \frac{\partial^2 q(t, x, y)}{\partial y^2} + F(t, x, y) \quad \text{where } g(t, x, y) \neq p(x, y)F(t)$$

This equation cannot be discretized with a single vector b . If this was discretized to be on the

form of (1.1) and solved with a projection method, it would look like:

$$\dot{u}(t) = Au(t) + \sum_{i=1}^{\hat{m}} e_i F_i(t),$$

where \hat{m} is the size of the matrix, and $F_i(t)$ is a time dependent function after spacial discretization. The reason for this is that every different point, x_i and y_i , gives a different time dependent function, and all of these functions need to be used to obtain the correct solution.

The reason the canonical vectors e_i are used is for simplicity, any set of orthogonal vectors can be used.

This means that equation (3.5.5) needs to be solved \hat{m} times to obtain the solution. This gives the projection methods a terrible run time. It is not advised to use any projection method if this is the case [12].

Operation	Cost
Integration with forward Euler	$\mathcal{O}(kn^2)$
Integration with Trapezoidal or midpoint rule	$\mathcal{O}(kn^3)$
Arnoldi's algorithm	$\mathcal{O}(n^2 \hat{m})$
Symplectic Lanczos method	$\mathcal{O}(n^2 \hat{m})$
Transforming from $z_n(t)$ to $u_n(t)$	$\mathcal{O}(\hat{m}nk)$
Matrix vector multiplication ($\hat{m} \times n$) (sparse matrix)	$\mathcal{O}(\hat{m})$
Matrix vector multiplication ($\hat{m} \times n$) (dense matrix)	$\mathcal{O}(n\hat{m}^2)$

Table 3.3: Computational cost of some mathematical operations. n is restart variable, \hat{m} is the size of the large matrix, and k is the number of steps in time. Numbers from this table is obtained from [16].

3.5.6 Number of operations

Since computation times might be uncertain due to different additional loads (web surfing, writing and so on) there will here be a short comparison between the number of operations for each method. This will also give a basis for what computationally complexities to expect from the different methods.

A table of computational cost for different operations is given in table 3.3.

Surprisingly the asymptotic cost for KPM and SLM is the same. A lot of small additional costs for SLM is hidden here meaning that KPM probably has a smaller computation time, but the computation times are increasing similarly. The windowing is also a wild card a since lot of costly operations are hidden. The difference between the projection methods and DM strongly depends on n and r_n , this makes it impossible to conclude anything without actually doing it, except that all methods are linear with k .

3.6 SLM and its eigenvalue solving properties

If you do a quick internet search of "symplectic Lanczos method" most articles you find are in relation to symplectic Lanczos method's ability to approximate eigenvalues of Hamiltonian matrices. This section I will try to explain what makes this algorithm so attractive for these types of problems. (This section is based on reading [5],[26], [6], and [15].)

Method	Explonation and number of operation
KPM	Arnoldi's algorithm, an integration method, and the transformation. $\mathcal{O}((n^2 \hat{m} + kn^3 + \hat{m}nk)i_r)$
SLM	Symplectic Lanczos method, an integration method and the transformation. $\mathcal{O}((n\hat{m}^2 + kn^3 + \hat{m}nk)i_r)$
DM	An integration method with $n = \hat{m}$. $\mathcal{O}(k\hat{m}^3)$
Windowing (KPM or SLM)	SLM or KPM needs to be run K times. $\mathcal{O}((n\hat{m}^2 + kn^3 + \hat{m}nk)i_r K)$

Table 3.4: Number of operations needed for the different methods with trapezoidal rule. i_r is the number of restarts needed for the method to converge. For windowing $K \cdot k$ is equal to k for the other methods. Windowing for DM is not interesting since it has exactly the same run time, and is exactly the same method.

The eigenvalue problem is found in many different areas, eg. control theory, model reduction, system analysis. No other algorithm that exploits the Hamiltonian structure and the sparsity of the matrices occurring in these areas.

SLM is a relatively fast algorithm for transforming big sparse Hamiltonian matrix to smaller sparse Hamiltonian matrix with similar properties. Eigenvalues of Hamiltonian matrices comes in pares, $\{\pm\lambda\}$, or in quadruples, $\{\pm\lambda, \pm\bar{\lambda}\}$. Since the small matrix is Hamiltonian, it is easier to find these pairs or quadruples. An other important property is that the biggest, and therefore often most important eigenvalue, are found first.

The method is not without its flaws. Frequent breakdown due to ill conditioned matrices occur. But due to its large potential much work has been made to overcome the difficulties. The most promising improvements are the different types of restarts. This way the numerical estimations can be improved without loosing the Hamiltonian properties, and without a too high cost. Unfortunately not all are very efficient. Though far from perfect, there is still much ongoing research on the topic.

An other method based on SLM is the SR - algorithm which has similarities with the QR - algorithm. SR applies symplectic operations to a Hamiltonian matrix instead of applying or-

thogonal operations as in QR.

Not all the papers are interested in improving the method, [15] shows under which assumptions the method converges.

Interestingly many of these papers also compare SLM to KPM.

Chapter 4

Practice

This section will be more concerned with programming choices, implementation, and how important data was calculated.

4.1 Outdata

This section will explain how different interesting values are calculated in the program.

All errors are obtained with the same function. At each time step, this function finds the maximum absolute difference between the approximated solution and the correct solution. The resulting vector of absolute errors is then divided by the correct solution, so that the error is relative to the correct solution. This will be marked with "error" on the plots. In the case where there is no correct solution, as in `semirandom`, the error is measured in relation to the solution without the projection method, marked with `errorcomp`.

The energy is found with one dedicated energy function. The exceptions are \mathcal{H}_3 and \mathcal{H}_4 which are calculated by a different function. The energy is calculated for each time step, and initial energy is subtracted. In the case where the energy is supposedly constant the energy is calculated without comparing it to anything. This is because the correct solution would sometimes have more energy than the approximation, making it difficult to draw any conclusions. This is done for all energies in section 5. When comparing approximated energy with analytical

energy, the energies are calculated independently, and then subtracted from each other. This is done for all energies in section 6. If the energies are compared to the analytical solution they are marked "energy", and energy^{comp} if DM and a projection method is compared.

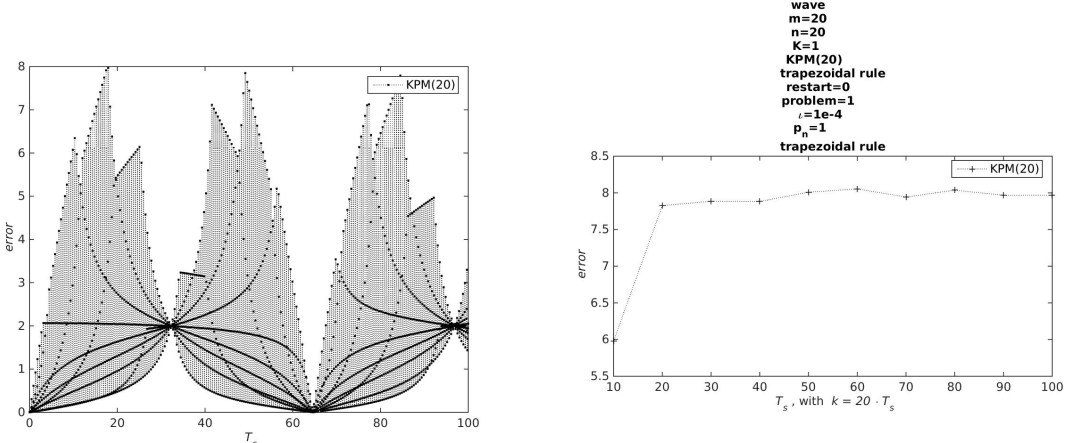
Other interesting results are the number of restarts performed and computation time.

Number of restarts are 0 if the projection method is not used, and 1 if the projection method is used without restart. Any restart is then counted and added to this. The reason for this is that when plotting the number of restarts on a logarithmic scale Matlab removes all negative numbers and zeros from the plot, which made some of the plots confusing. The symbol for the number of restarts will be i_r .

Computation times are measured as the time for the actual computation of the problem to be completed. Initial computations, or plots is not counted, as these are common for both the projection methods, and the direct method. The symbol for computation time is T_c .

4.2 Pictures

All pictures are plotted with a dedicated plot tool. This makes it easier to change plots, or uncover programming faults. The greatest absolute values of energy or error are the points used in plots. This is made possible by running the solving program once for each point. This removes noisy data from the figures, and also makes it possible to make the points look equally spaced on logarithmic plots. In figure 4.1 the difference between the two is shown.



(a) A plot made by a single run with the solution program.

(b) A plot made by running the solving program one time for each point, and then using the maximum of those values in the plot.

Figure 4.1: These pictures show how removing useless data can make the pictures easier to understand. The picture on the left shows the error for all time steps. The picture on the right shows the maximum error from start to each point.

4.3 Test problems

Equation (1.1) can be the result of several discretized equations. Since SLM needs a Hamiltonian matrix this will be the main focus. Two different matrices is implemented. These matrices also have their two test problems. All test problems satisfies the condition

$$u(t, 0, y) = u(t, 1, y) = u(t, x, 0) = u(t, x, 1) = 0.$$

The discretization is done by dividing each spacial direction, $[0, 1]$ in m pieces, with step size $h_s = 1/m$, so that $y_i = i h_s$, $x_i = i h_s$ with $i = 1, 2, \dots, m - 1$.

4.3.1 The wave equation

The first test problem is the 2 dimensional wave equation,

$$\frac{\partial^2 u}{\partial t^2} = \frac{\partial^2 u}{\partial x^2} + \frac{\partial^2 u}{\partial y^2} + p(x, y)f(t). \quad (4.1)$$

To obtain the matrix, approximate $\frac{\partial^2 u}{\partial x^2} + \frac{\partial^2 u}{\partial y^2}$ with \tilde{A} , where \tilde{A} is the five point stencil[17]. Then

write it as a system of first order (in time) differential equations

$$\begin{aligned}\dot{q}(t) &= Iw(t) \\ \dot{w}(t) &= -\tilde{A}q(t) + \tilde{b}\tilde{F}(t).\end{aligned}\tag{4.2}$$

Now, let $u(t) = [q(t); w(t)]$, $bF(t) = [0; \tilde{b}\tilde{F}(t)]$, and

$$\begin{aligned}\tilde{A} &= \frac{2}{h_s^2} \text{ gallery('poisson', } m-2) \\ A &= \begin{bmatrix} 0 & I_{\hat{m}} \\ -\tilde{A} & 0 \end{bmatrix},\end{aligned}\tag{4.3}$$

where A is a Hamiltonian matrix. This matrix will be referred to as wave, and is a second order approximation of the wave equation.

Two test problems will be used to check the integrity of the program. One with constant energy, and one with varying energy.

In the case when the energy is constant the test problem is

$$\begin{aligned}q(t, x, y) &= \sin(\pi x) \sin(2\pi y) \cos(\sqrt{5}\pi t) \\ w(t, x, y) &= \sin(\pi x) \sin(2\pi y) \sqrt{5}\pi \sin(\sqrt{5}\pi t) \\ q_0(x, y) &= \sin(\pi x) \sin(2\pi y) \\ w_0(x, y) &= 0 \\ f(t, x, y) &= 0.\end{aligned}\tag{4.4}$$

For varying energy, it is

$$\begin{aligned}q(t, x, y) &= \sin(\pi x) y(y-1)(t^2 + 1) \\ w(t, x, y) &= \sin(\pi x) y(y-1)(2t) \\ q_0(x, y) &= \sin(\pi x) y(y-1) \\ w_0(x, y) &= 0 \\ f(t, x, y) &= 2 \sin(\pi x) y(y-1) - (t^2 + 1) \sin(\pi x) (2 - \pi^2 y(y-1)).\end{aligned}\tag{4.5}$$

Both q and w are used when measuring the error.

4.3.2 A random test problem

The second implemented Hamiltonian matrix is random, and given by

$$\begin{aligned} D &= \text{rand}(\hat{m}, 1) + 5I_{\hat{m}} \\ D1 &= \text{rand}(\hat{m} - 1, 1) \\ A &= \text{gallery('tridiag', } D1, D, D1) \end{aligned} \tag{4.6}$$

Since we are interested in comparing the different projection methods to each other, the matrix will be saved and reused. This matrix will be referred to as `semirandom`. The part $5I_{\hat{m}}$ is added to make $J_{\hat{m}}A$ diagonally dominant, since a fully random problem will not converge in general. The matrix is simulated as a 2 dimensional system. Since the projection methods are only usable with sparse matrices, it is tridiagonal.

The test problem is given by

$$\begin{aligned} u(t, x, y) &= \text{unknown} \\ \dot{u}(t, x, y) &= \text{unknown} \\ u_0(x, y) &= \text{rand}(2(m - 2)^2, 1) \\ f(t, x, y) &= 0 \end{aligned} \tag{4.7}$$

when the energy is constant, and

$$\begin{aligned} u(t, x, y) &= \text{unknown} \\ u_0(x, y) &= 0 \\ f(t, x, y) &= \text{rand}(2(m - 2)^2, 1) \cdot \text{rand}(1, k), \end{aligned} \tag{4.8}$$

when the energy is varying.

Since the solutions to the test problems are unknown, it is impossible to show convergence in the traditional sense. A larger m does not give a better approximation of some equation, it

gives a new matrix, with no relation to any matrix with different m . This test problem might therefore seem uninteresting, but there are some reasons to use it. It gives a tridiagonal Hamiltonian matrix with much randomness, making it difficult for the projection methods to find an approximated solution, while `wave` always has the same matrix. This case will also show more correctly how the restart can be used to improve the solution than `wave` will.

The error will in this case be measured as the difference between the projection method and DM, it will be marked $\text{error}^{\text{comp}}$. This will make the error seam a lot smaller than it really is, but as shown in section 3.5.4, it is correct to compare the solutions in this manner. When the energy is constant there is no need to do anything different, but varying energy will be compared with its non-projected equivalent.

4.4 Implementation

All algorithms and methods is implemented in matlab R2014b on an ubuntu 14.04 LTS computer with intel i7 4770 CPU and 16 GB of RAM.

The program was divided into several small functions that were tested individually. Functions are reused as much as possible. Matlab's backslash operator was used to solve the linear system in trapezoidal rule and midpoint rule.

There are two ways to implement the number of restarts the projection methods should perform. One way is to choose a number of iterations and hope it converges. The other method is to iterate until the change in the solution is below a certain threshold tolerance. Both of these methods are implemented, but mostly the last will be used since this gives more information about how well the solution is approximated. The tolerance will be called ι (iota) since it is used to describe something small, and both ϵ and δ were unavailable [4].

Chapter 5

Results for test problems with constant energy

This chapter will show how error and energy changes with i_r , ι , T_s , m and n . There are special interest in seeing how the energy for SLM behaves, how KPM and SLM differs, and how problems might be handled. The predictions and proofs made in the theory chapter will also be tested.

For all sections except the first assume that $m = 20$, and $k = 20$ per second.

5.1 Convergence

This section will show convergence with the wave equation with all the integration methods presented in table 3.1 and 3.2. The reason for only using the wave equation is that the analytical solution is unknown for semirandom, and increasing m does not give a better approximation of the method, it gives a different problem all together. $T_s = 1$ second for all plots in this section.

5.1.1 Numerical integration

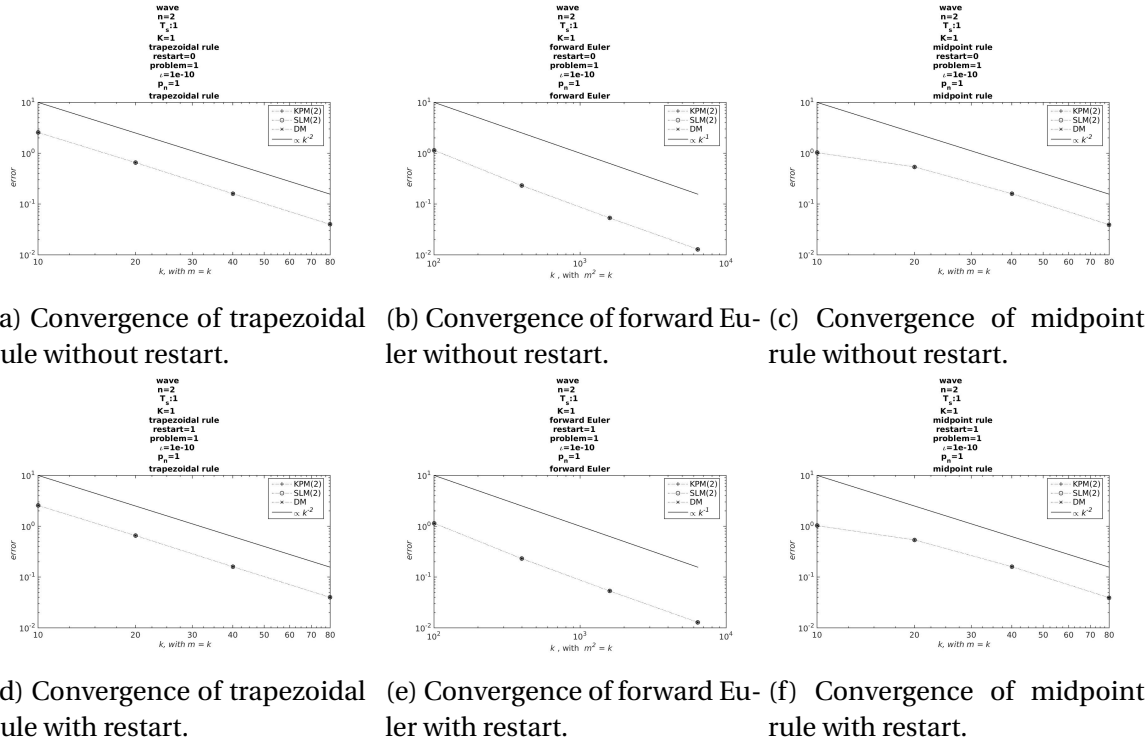


Figure 5.1: Figure of the convergence for the different integration methods. Notice that forward Euler uses k^2 where the other methods uses k to obtain the same accuracy. $n = 2$ is kept constant for all plots, since smaller n generally gives poorer convergence. For the figures with restart enabled $\iota = 1e - 10$. 1 second is simulated.

All methods converge with the expected rate.

Forward Euler has a worse run time than the other methods, due to the larger k needed for the same convergence. It also has a tendency to diverge on longer time intervals and is in general not suited for the job. Figure 5.2 shows the difference in energy between forward Euler(5.2a) and trapezoidal rule (5.2b). This difference in energy is reason enough not to use forward Euler any more.

Trapezoidal rule and midpoint rule converges quadratically and near identically, as they should. Since midpoint rule is symplectic, it will be used when restart is enabled. Trapezoidal rule has a faster run time, and will be used when restart is not enabled, since midpoint rule and

trapezoidal rule is the same in this case.

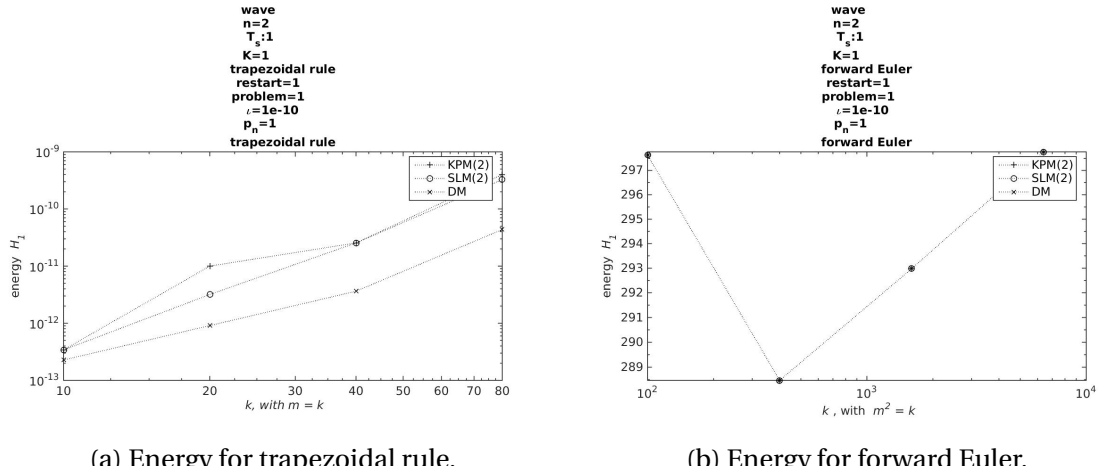
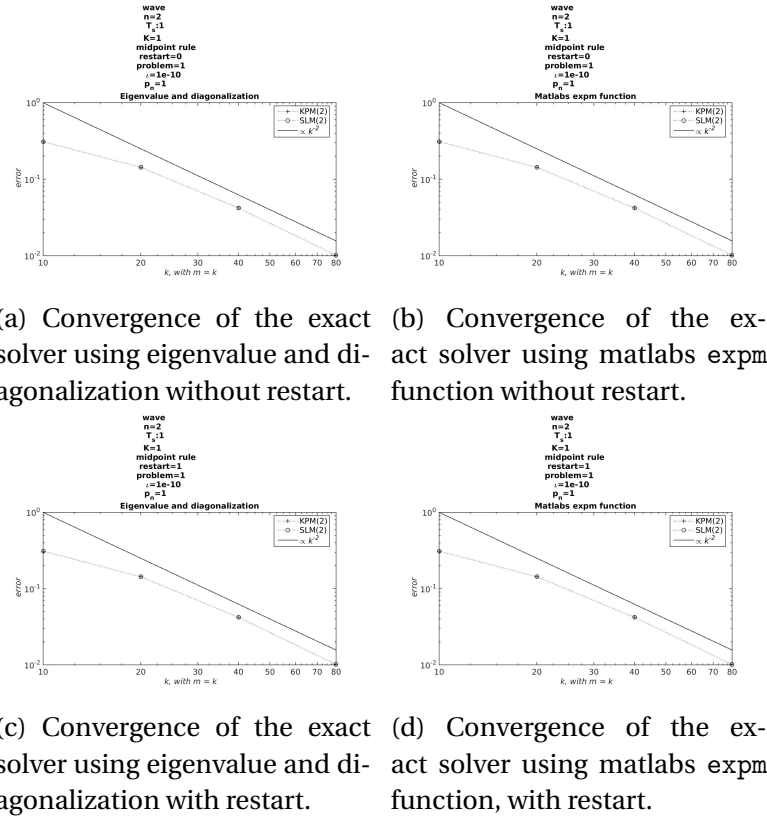


Figure 5.2: A figure showing the difference in energy between trapezoidal rule and forward Euler when 1 second is simulated.

5.1.2 Exact solvers



(a) Convergence of the exact solver using eigenvalue and diagonalization without restart. (b) Convergence of the exact solver using matlabs `expm` function without restart.

(c) Convergence of the exact solver using eigenvalue and diagonalization with restart. (d) Convergence of the exact solver using matlabs `expm` function, with restart.

Figure 5.3: Convergence for exact solvers, with midpoint rule for the restarts. Note that the exactness of the methods are for the integration in time, and not the spacial discretization. The expected convergence is therefore still quadratic. $n = 2$ because taking the matrix exponential is a costly operation and it is harder for the methods to converge when n is small. When restart is enabled $\iota = 1e - 10$. 1 second is simulated.

The convergence is quadratic and identical for both integration methods. It might seem strange to include two different exact solvers which look so similar, but an important difference between the two explored in section 5.7.1.

5.2 Convergence with the restart

In this section the correlation between ι and i_r , and how error and energy changes with this will be examined.

5.2.1 convergence as a function of ι

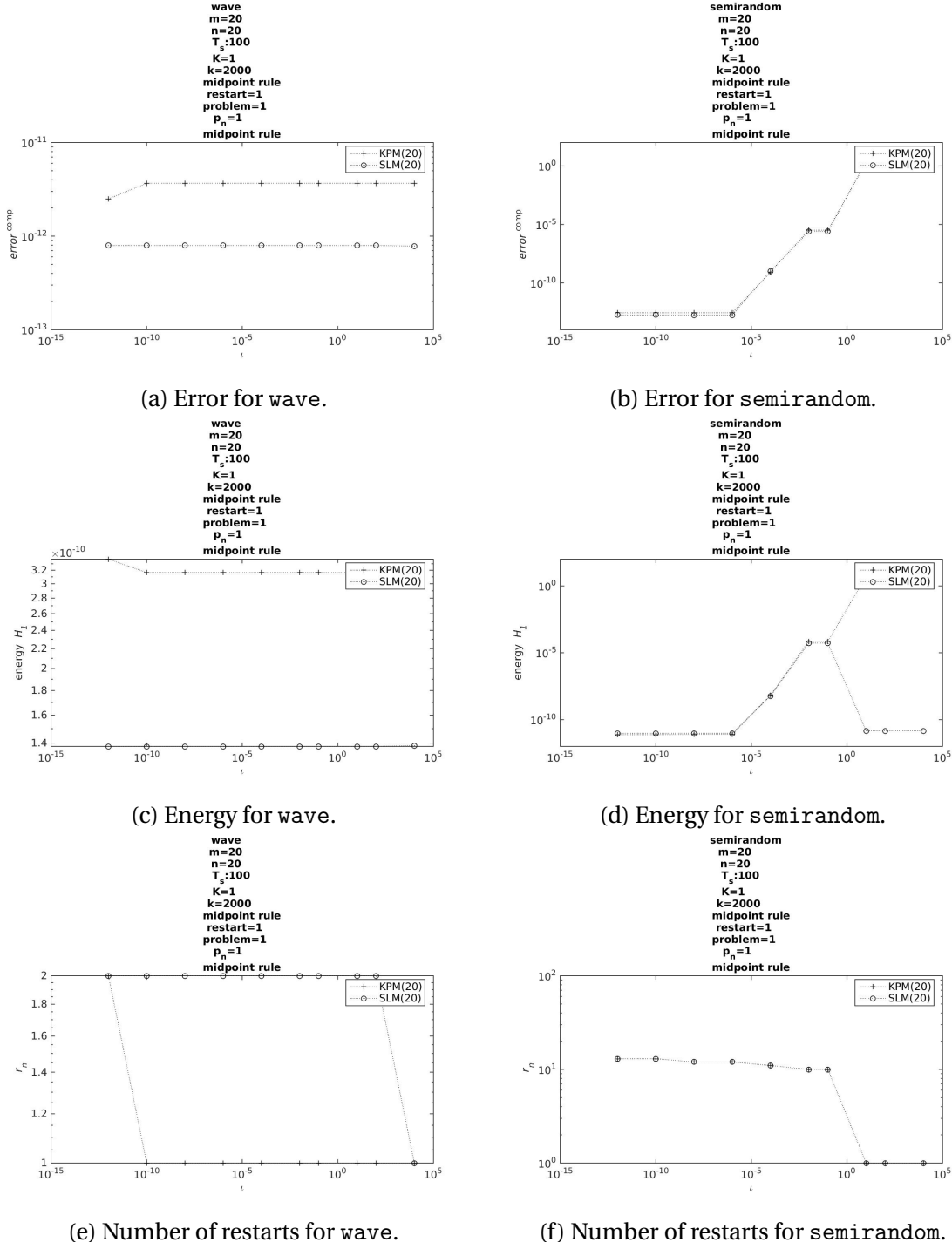


Figure 5.4: These figures show how choosing the correct ι can improve the solution, but also make the program run slower due to excessive restarts. The pictures on the left is for **wave** and on the right for **semirandom**. This plot considers 100 seconds, with $k = 2000$, $n = m = 20$ and midpoint rule is used.

Figure 5.4 shows that if `wave` is used there is no reason to use the restart. From figure 5.1 it seems to also be the case for larger m . This will therefore be the end of the discussion about `wave` in this chapter. The rest of this chapter will only consider `semirandom` since this is a more interesting case.

The number of restarts are the same for KPM and SLM. Another thing to notice is that there is little reason to restart after gaining a certain precision, since the changes will not be visible. ι should be chosen a few orders smaller than the accuracy of DM. Based on the pictures $\iota = 1e-6$ will work nicely.

Some interesting results from 5.4d and 5.4b is that both KPM and SLM needs to restart to gain a low error, but the energy for SLM increases the first times it restarts, before it starts sinking again. This shows that the energy can be accurately estimated by SLM without restart, but not (necessarily) the error. Thus it is clear that SLM loses its energy preserving property when it restarts. If only the energy is of interest, the restart is not necessary. For KPM it is much simpler, more restart means better approximations, of both error and energy.

5.3 Convergence with i_r

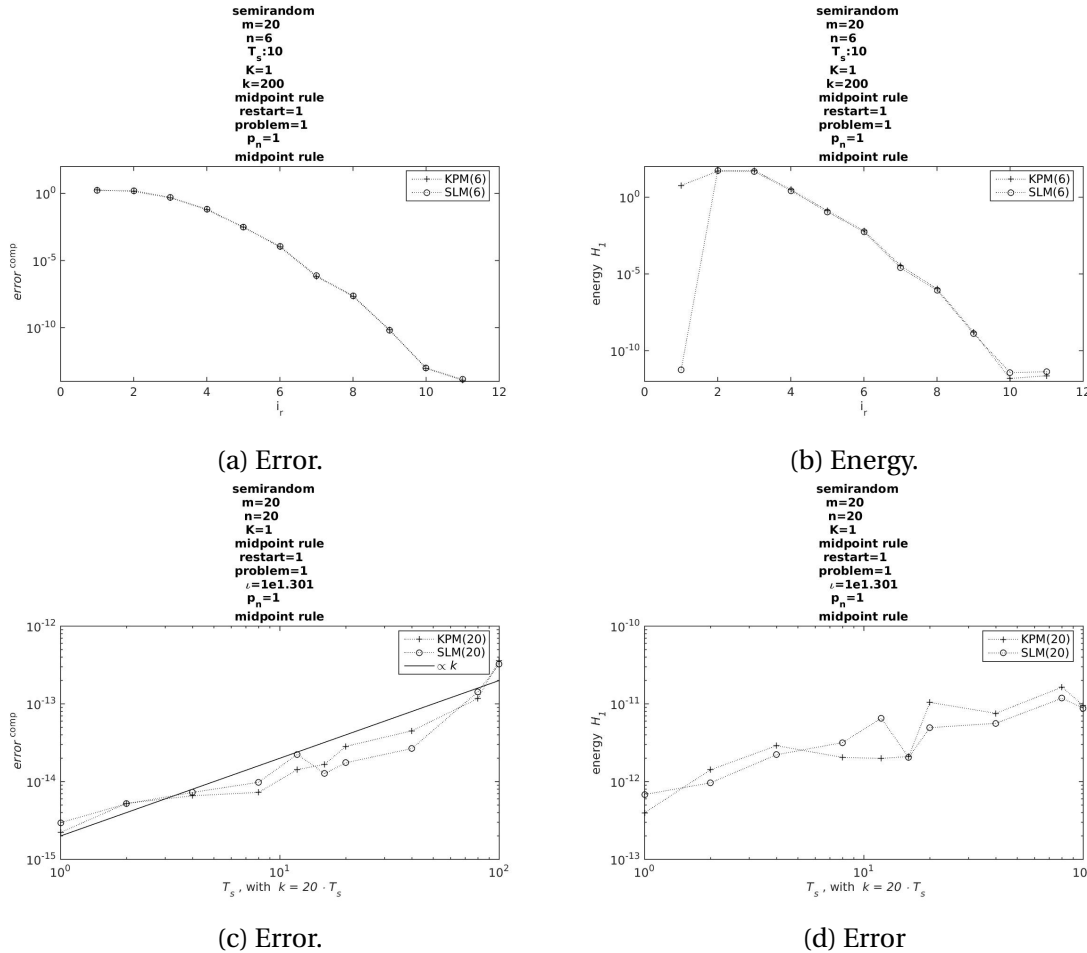


Figure 5.5: The top figures shows how the error and energy changes as a function of i_r . The numbers $n = 6$ and $T_s = 10$ is chosen to better show the decrease. For i_r larger than 10 there are no change in the plot, larger n gives a quicker convergence. The bottom pictures show how error and behaves with increasing time domain, with $i_r = 20$. Values are chosen to make the method work.

Figure 5.5 shows that a few restarts are needed before a better approximation is made. After a certain number of restarts the change in the solution is too small to observe.

The increase in error is linear for 5.5a, which is what is predicted for these methods. The increase is close to constant when ι is chosen instead of i_r .

The increase in energy is sub linear. It was predicted that it would be constant for SLM. Why the increase happens will be examined later in this chapter.

5.4 How to choose n

This section will look at how to choose n , to avoid unnecessary restart and still obtain satisfactory results. Last section show that error and energy behaved quite similarly. Thus this section will only show error, since this is the most important property of the restart. We assume that all cases tested here are independent.

5.4.1 Without restart

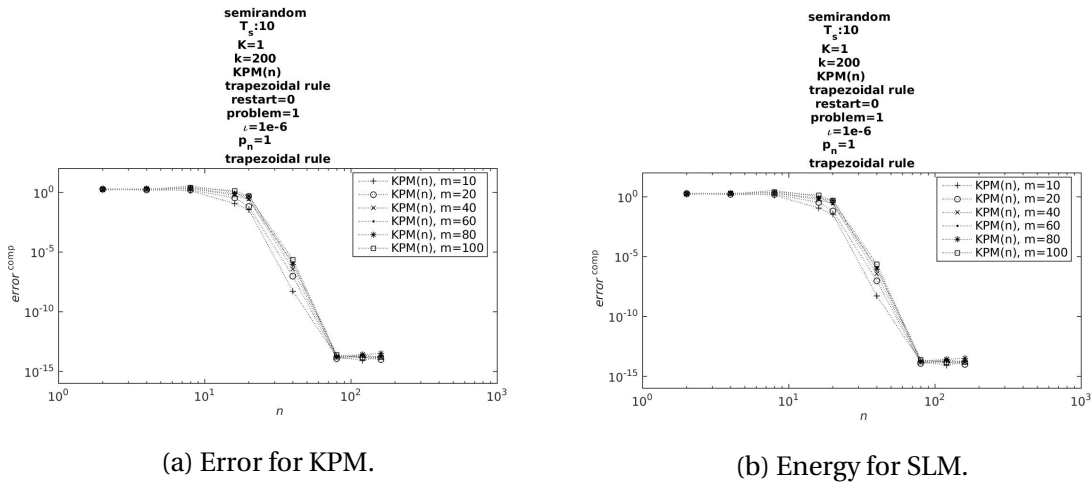


Figure 5.6: The pictures shows which n gives convergence for different m when restart is not enabled. This plot is made with trapezoidal rule with $k = 200$ over 10 seconds.

Figure 5.6 shows that n can be choose nearly independent of m , as long as $n \geq 100$ and restart is not enabled.

5.4.2 With restart

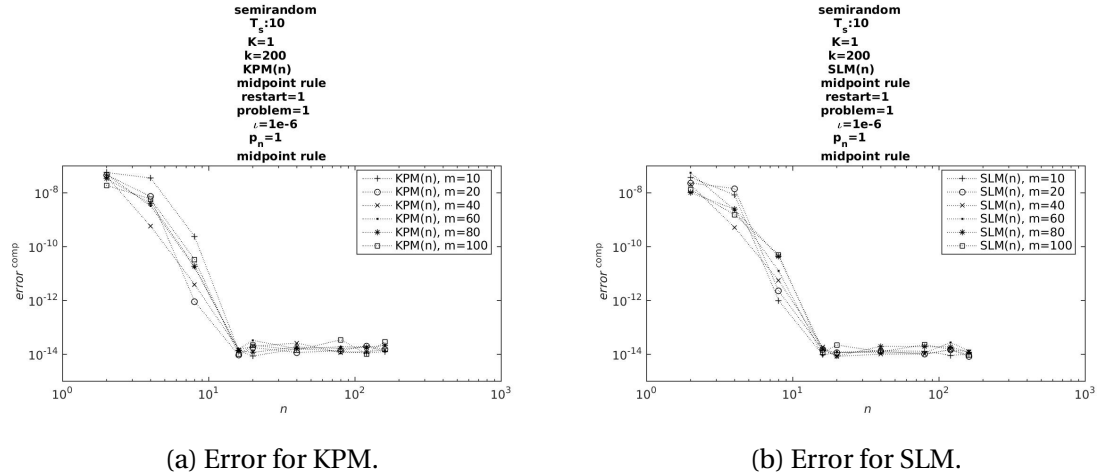


Figure 5.7: The pictures shows which n gives convergence for different m when restart is enabled. This plot is made with midpoint rule with $k = 200$ over 10 seconds.

Figure 5.7 shows that if restart is enabled, a good approximation of the solution can be found with $n \geq 20$, for any m .

The reason for the independence between m and n is probably due to the structure of the matrix, and is not a rule for the general Hamiltonian matrix.

5.4.3 For time domains

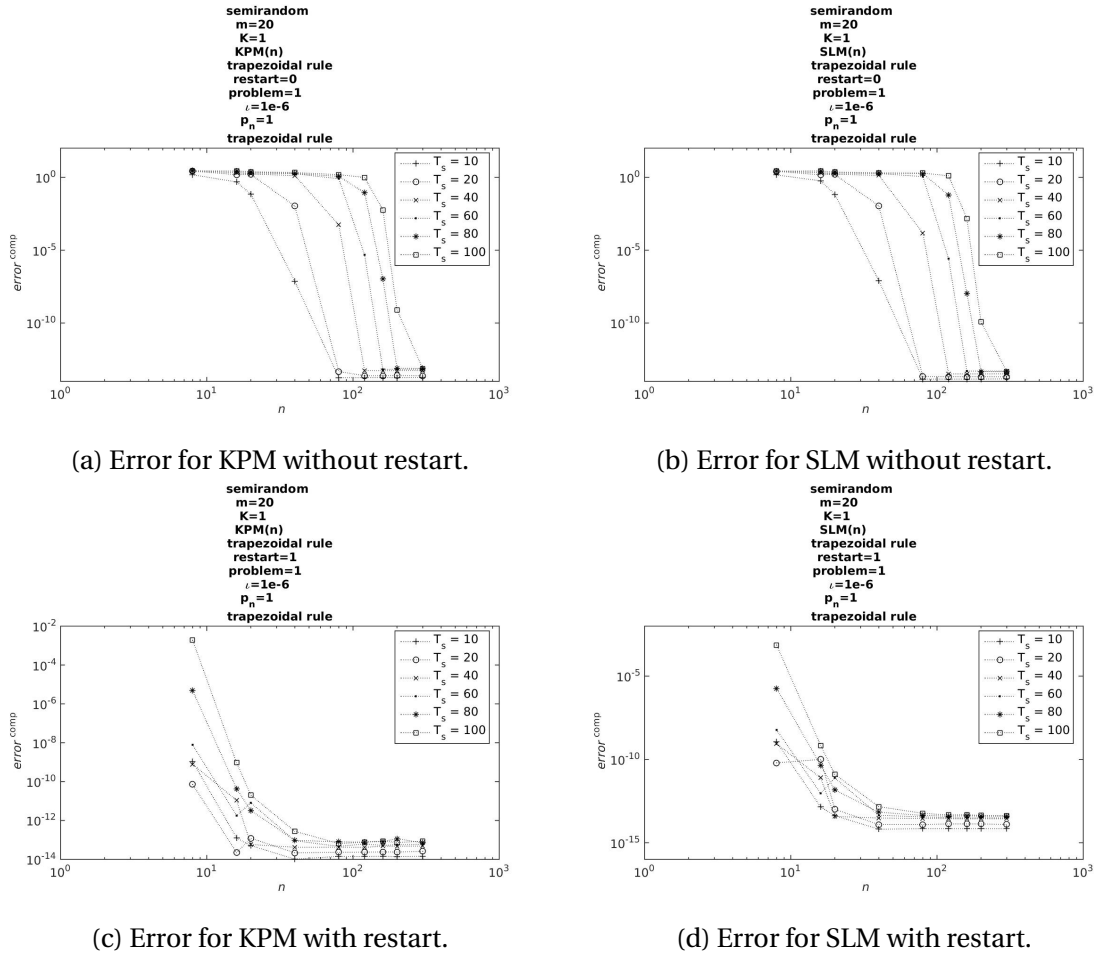


Figure 5.8: The pictures shows which n gives convergence for different T_s , with $k = 20 \cdot T_s$. The top plots are without restart, and the bottom with restart. This plot is made with trapezoidal rule with $k = 200$ over 10 seconds.

Figure 5.8 shows that the length of the time domain is affecting the choice of n . It seems that if T_s is doubled, then n needs to be doubled. Though this rule seems to be less important when restart is enabled.

SLM and KPM behaves very similarly in all pictures shown in this section.

5.5 Energy and error

The convergence section shows that increasing m and k will decrease the error of the solution. This has been done for short time (1 s). Convergence for the restart has also been shown both for

different i and i_r . There has also been a discussion about how to chose n . The values of these will be kept at $n = 200$ when restart is not used. $n = 20$ and $i = 1e-6$ when restart is used. Remember that $m = 20$ except where stated. This section will look at how error and energy change as a function of time, and how the restarting and windowing interacts with this.

Without restart

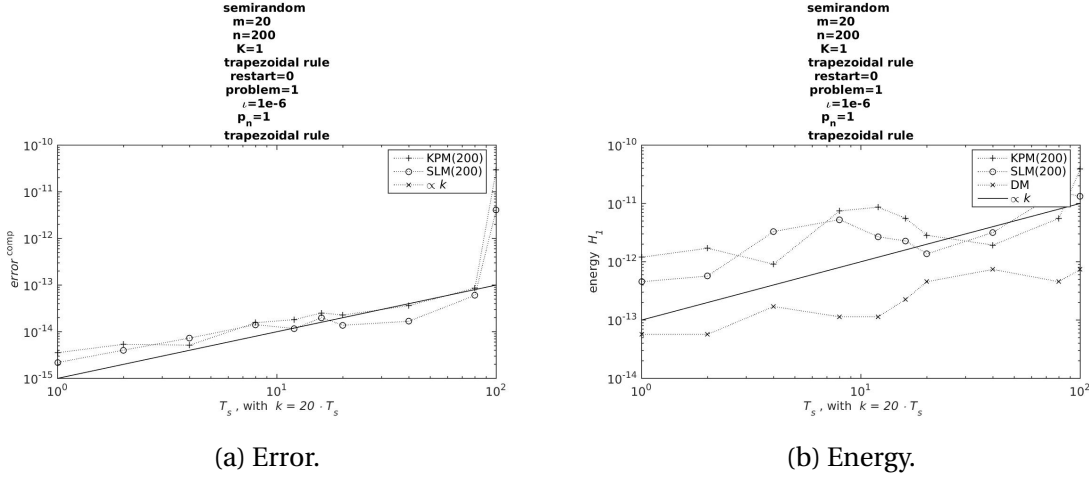


Figure 5.9: The figures show how error and energy changes with larger time domains. $n = 200$ is chosen based on the figures in section 5.4. $m = 20$, and trapezoidal rule is used.

The energy and error for all methods increase, but slower than linear, and might be explained by small rounding errors that cannot be avoided when dealing with such small numbers.

The suddenly increase in error at the last point in figure 5.9a shows the instability of the projection methods, this also happens when restart is enabled, and will be explained further in section 5.5. If the time domain was a little larger the projection methods would diverge.

With restart

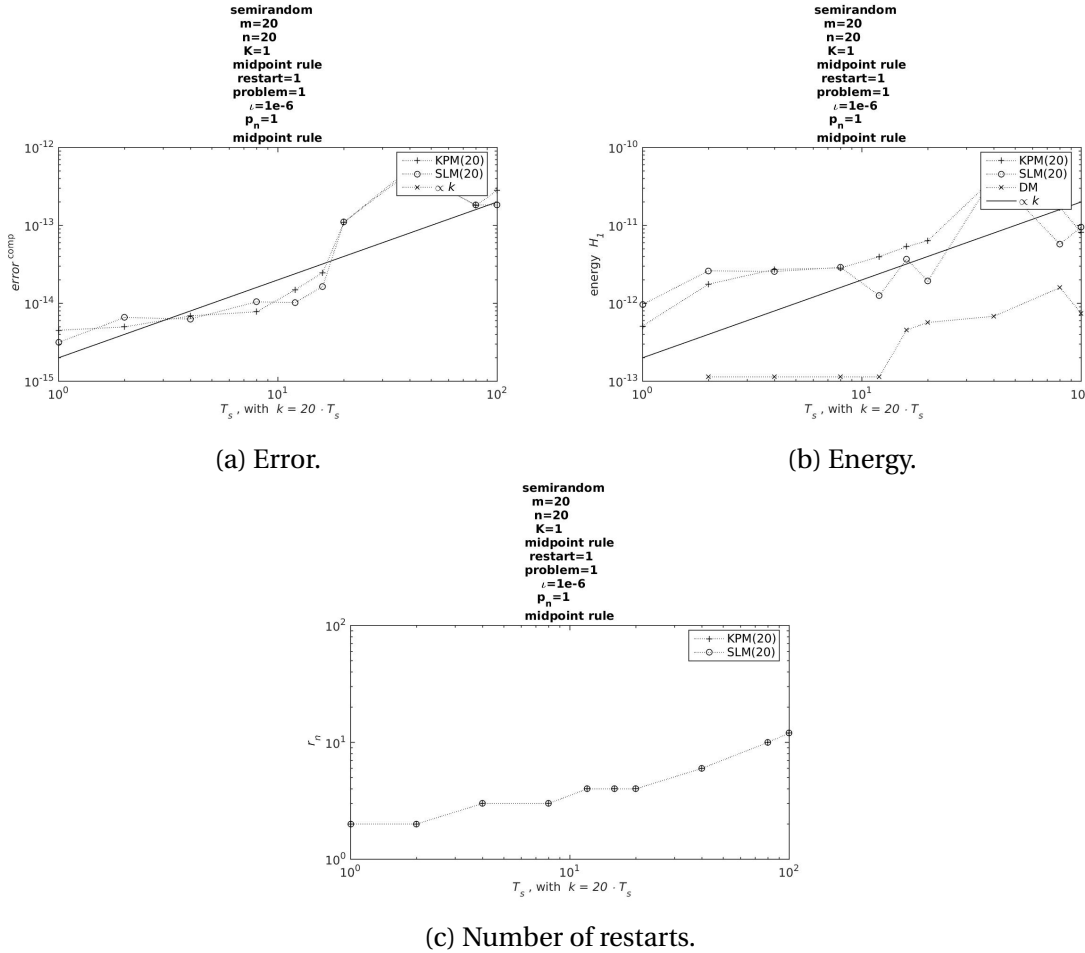


Figure 5.10: The figures show how error and energy changes with larger time domains when restart is enabled with $\iota = 1e - 6$. $n = 20$ is chosen based on the figures in section 5.4. $m = 20$, and midpoint rule is used.

Figure 5.10 and 5.9 are quite similar. The main difference is of course that restart is enabled in figure 5.10, and $n = 20$, instead of $n = 200$ as in figure 5.9. Which of these methods are most desirable will not become apparent before computation time is discussed.

The number of restarts increases linearly after the time domain has become sufficiently large. Larger time domains might therefore give a larger growth in computation time than linear.

Windowing

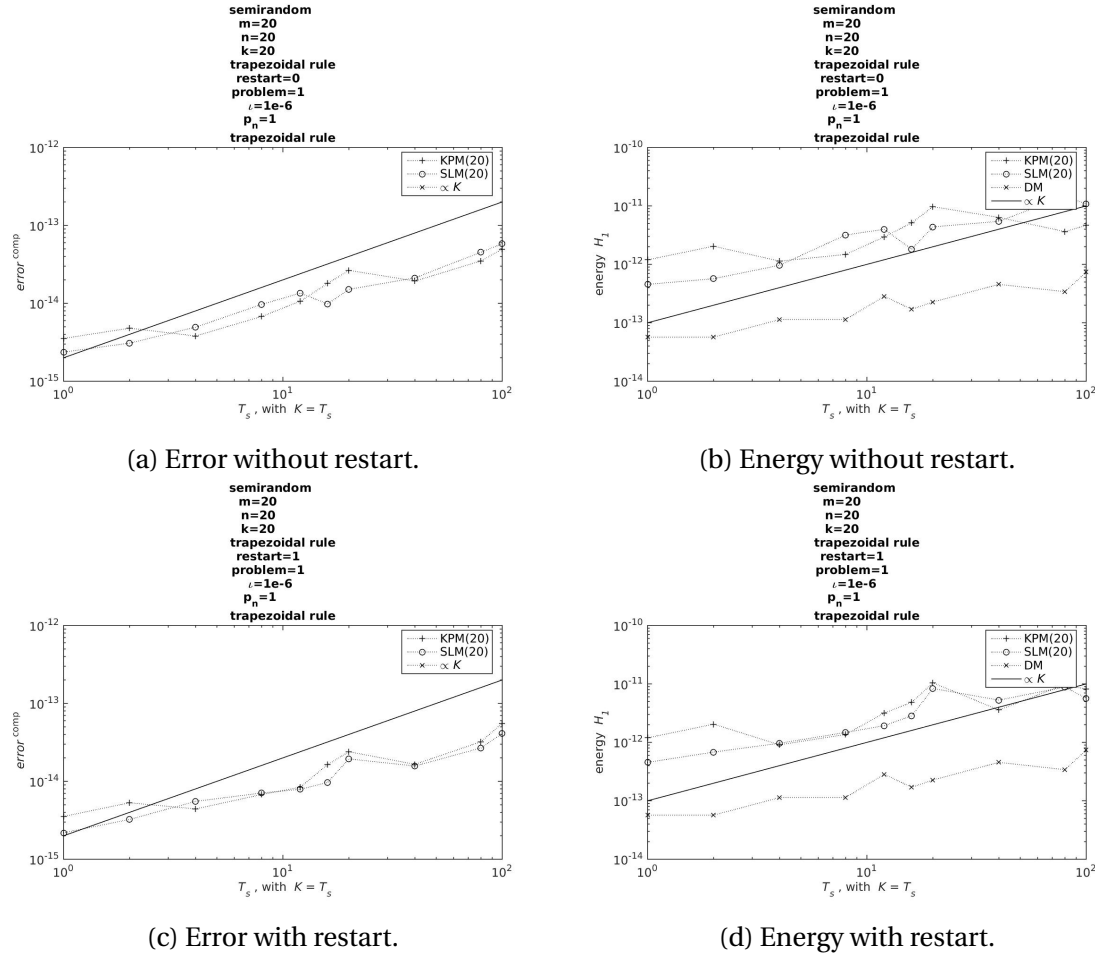


Figure 5.11: The figures shows how windowing with and without restart changes the error and energy over time. $m = 20$, $k = 20$ and $\iota = 1 - 6$ when restart is enabled.

In this case the restart does not seem to matter. The error and energy is the best yet, though it still increases close to linearly. Ideally the error and energy would be close to constant. Windowing is clearly an interesting idea.

Very long time

In this section it is shown what will happen when the time domain becomes to large for the methods to converge.

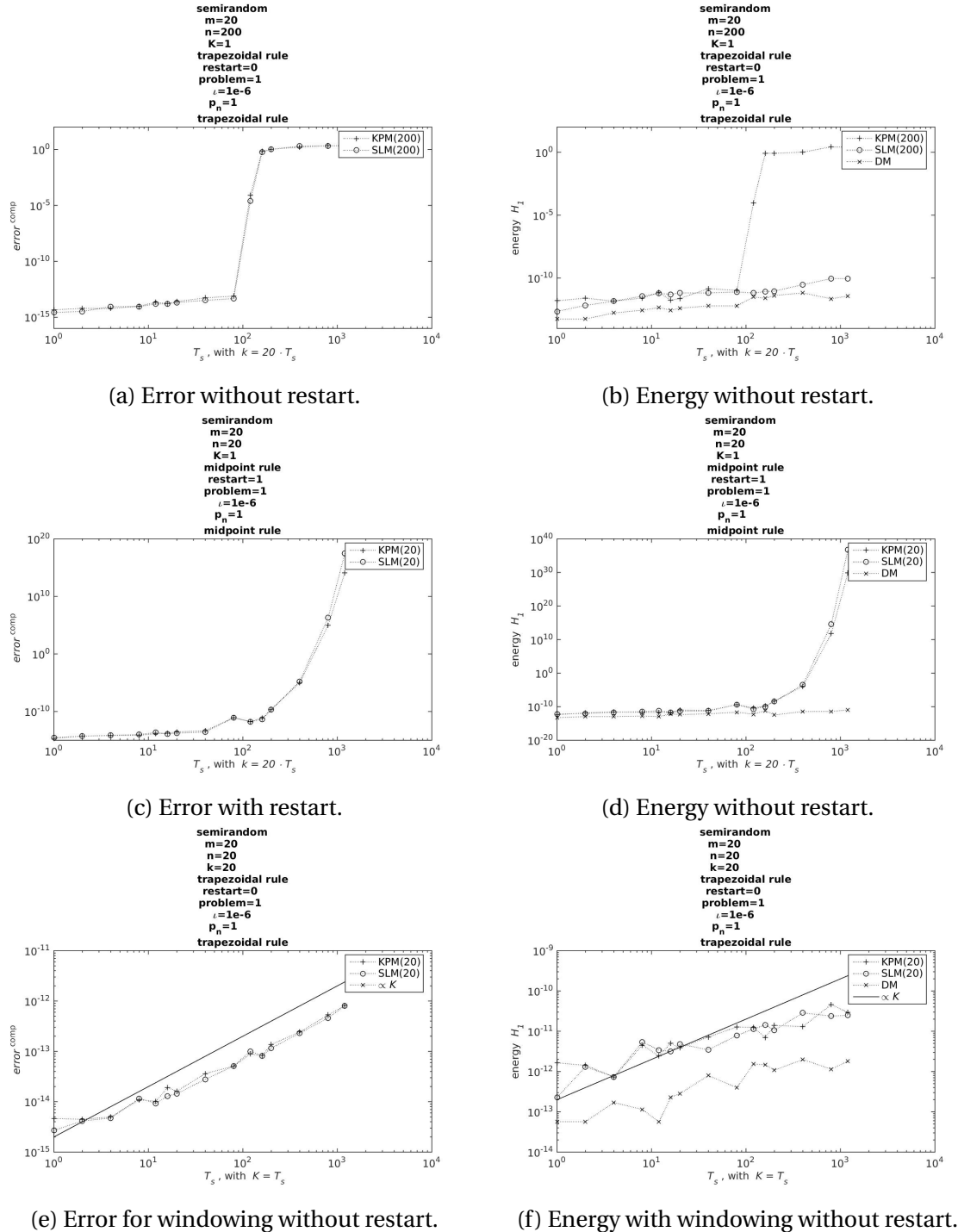


Figure 5.12: This figure shows how different methods cope with a very long time domain. Windowing does not use restart since there are so little difference.

This figure shows something very interesting, namely that with restart or not, the methods will diverge on long time domains if n is kept constant. There is an important difference be-

tween the two methods. If restart is not enabled, the method will at one point not work, and the energy and error will just be noise. But the numeric value of the approximated solution will be close to the numeric value of DM. With restart on the other hand everything blows up exponential. When windowing is used the problem can be worked around. In this case the trend of increasing energy and error continues as it did for 100 seconds.

Energy in the transformations

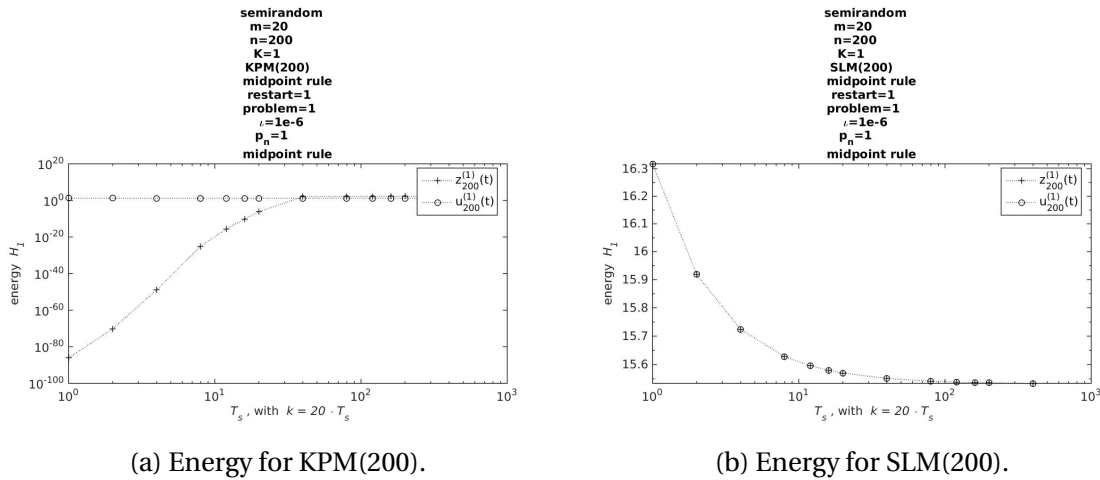


Figure 5.13: The figures shows how the transformation between $z(t)$ and $u(t)$ changes the energy. Restart is not enabled, $m = 20$, and trapezoidal rule is used.

For KPM there is a huge discrepancies between the energy of $z_n^{(i)}(t)$ and $u_n^{(i)}(t)$. For SLM there is no difference between the two. This shows the energy preserving properties of SLM. It is worth mentioning that $S_n J_{\hat{m}} S_n - J_n \sim 1e-16$ and $V_n^\top V_n - I_n \sim 1e-11$.

5.6 Residual energy

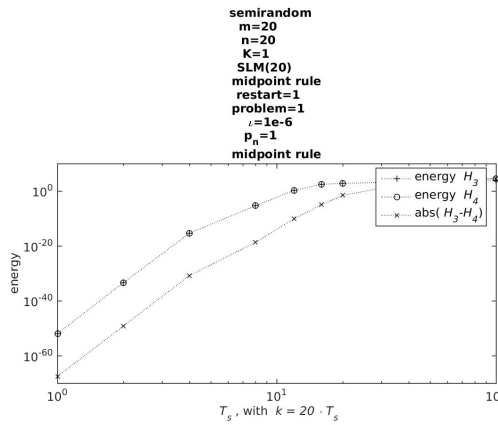


Figure 5.14: A plot of \mathcal{H}_3 and \mathcal{H}_4 for different time domains.

\mathcal{H}_3 and \mathcal{H}_4 are very similar, as is predicted in the theory section. The difference between the two is machine accuracy until T_s gets to big.

5.7 A different idea

This section will see how using an exact solver can improve error and energy, compared to trapezoidal and midpoint rule.

Unfortunately the test problems has some severe limitations. `wave` does not require a restart to get a well approximated solution, and the analytical solution is unknown for `semirandom`.

If `wave` is used the question about whether to use restart or not will remain unanswered. If `semirandom` is used there will be no way of knowing if DM or the projection method gives the most correct solution.

`wave` will be used for this since the solution is expected to be close to the analytical solution. Restart will not be used since it is already known that the method will not restart. Thus the question about whether to use restart or not with an exact solver will not be answered in this text.

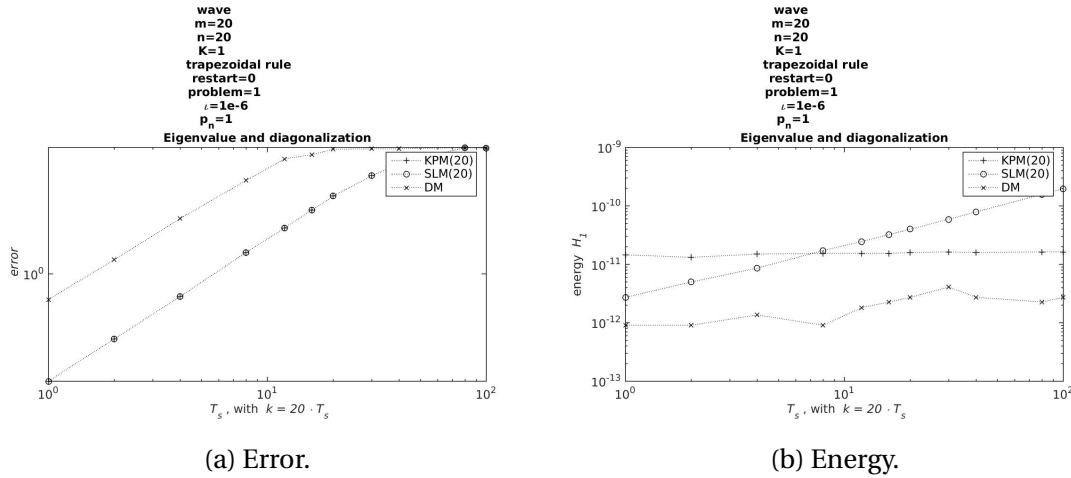


Figure 5.15: A figure showing how the error and energy changes when an exact solver(eigenvalue and diagonalization) is used. $n = 20$, $m = 20$.

The error for the projection methods with an exact solver is smaller than the error for DM with trapezoidal rule.

The energy for SLM increases linearly, why this happens is unknown. For both KPM and DM the energy is constant. It seems that KPM is better than SLM in this setting.

5.7.1 Matlabs expm function

This section will explain the reason for using eigenvalue and diagonalization instead of `expm`.

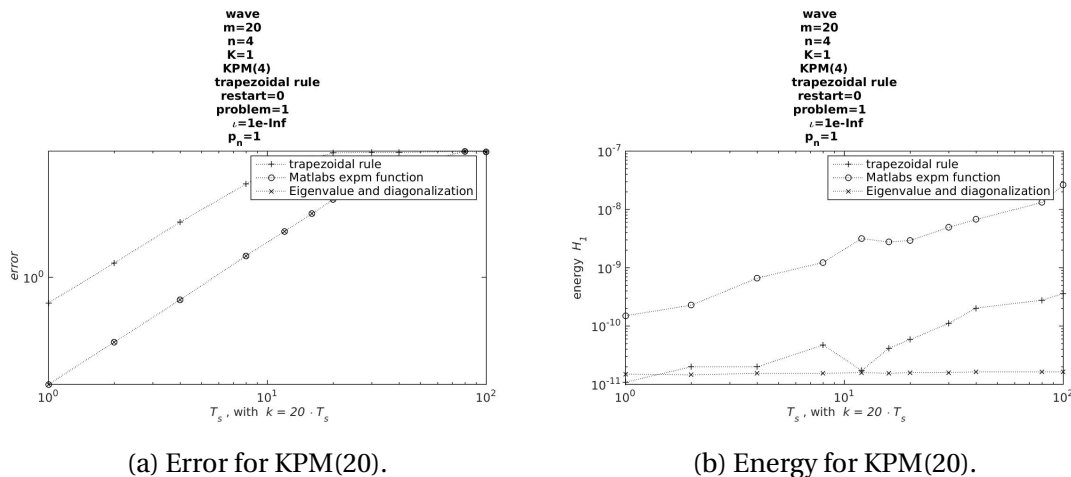


Figure 5.16: A figure showing the difference in error and energy for the different exact integration methods. Restart is not enabled, $m = 20$.

There are little difference in error between the exact solvers. Trapezoidal rule increases equally fast, but has a much larger initial error.

There is a big difference between the two exact solvers in energy. Eigenvalue and diagonalization has a constant energy, while trapezoidal rule increases half as fast as `expm`, which increases linearly.

This is an important reason to not to use `expm` when doing these calculations, since they counteract the most important properties of SLM.

5.8 Computation time

This section will compare the computation time for the different methods discussed.

5.8.1 Without restart

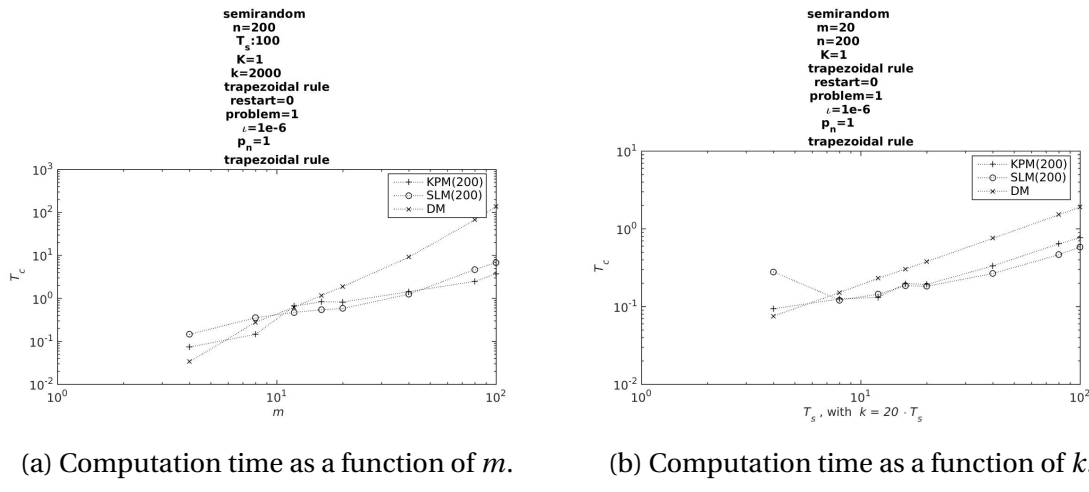


Figure 5.17: A figure of the computation times without restart with $n = 200$, $T_s = 100$, $k = 2000$, $m = 20$.

All computation times scales linearly with k , but SLM and KPM require much less computation time than DM.

The scaling with m is a little more difficult, but DM seams to be increasing quadratically, while SLM and KPM increases closer to linear. SLM and KPM has very similar computation times.

5.8.2 With restart

Since n can be chosen freely above a certain threshold, but smaller n might give higher i_r , it is interesting to see how computation time and n scales. When restart is not enabled it is quite obvious that smaller n gives smaller computation times.

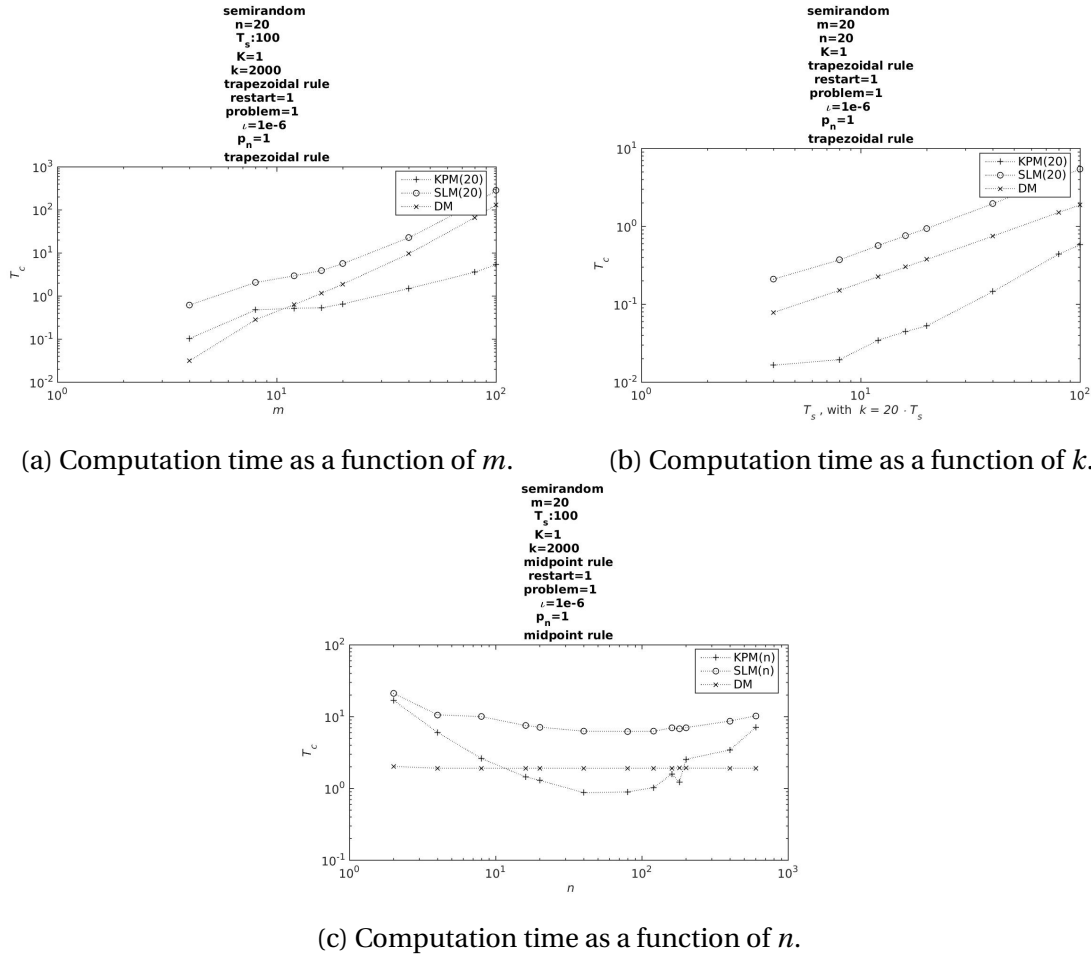


Figure 5.18: The top pictures show the computation times with restart, $n = 20$, $T_s = 100$, $k = 2000$, and $m = 20$. The bottom picture shows how computation time changes with n .

SLM and DM is now increasing equally fast with m , while KPM increases about the same as before. In this case DM would be a better choice than SLM, while KPM at least gives a smaller computation time.

The scaling with k for KPM increases faster than the others. This is because KPM needs more restarts with larger time domains. It would be interesting to see if this effect continues with

larger k and T_s . For SLM this effect is not visible.

5.8.3 Windowing

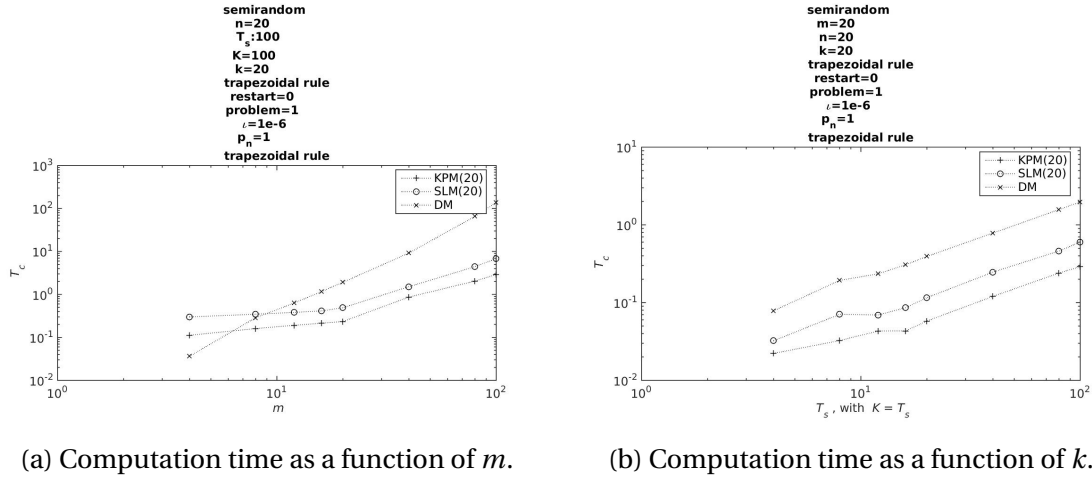


Figure 5.19: A figure of the computation times with restart, $n = 20$, $T_s = 100$, $k = 20$ per second, and $m = 20$.

Windowing gives the best performance for SLM and KPM till now. It is interesting that this method gives the best estimates for error and error, and the fastest computation time. The reason for the faster computation time is probably the small n without the need to restart.

5.8.4 With expm

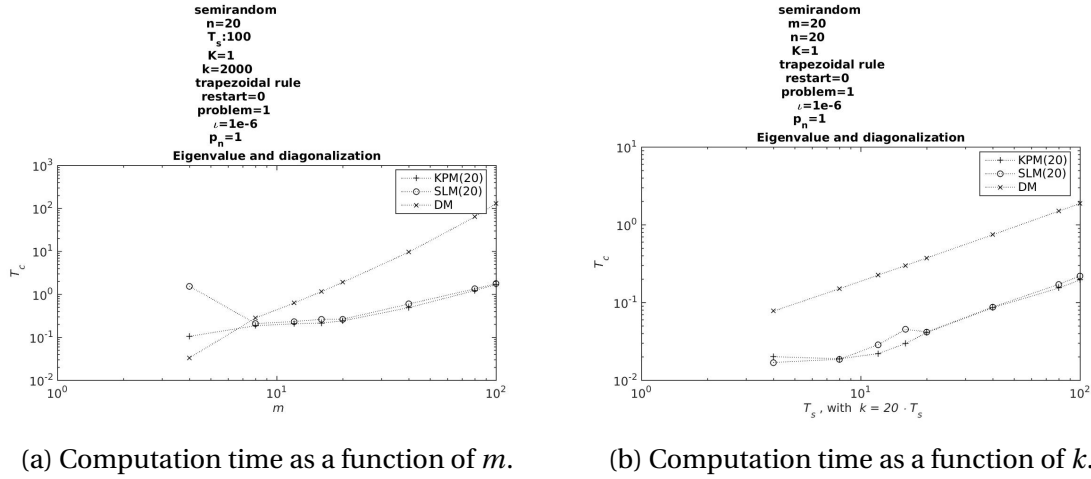


Figure 5.20: A figure of the computation times with Eigenvalue and diagonalization with $n = 20$, $T_s = 100$, $k = 2000$, $m = 20$.

Figure 5.20 shows that the exact solver without restart is even faster than windowing. If Windowing was used with this time integration methods all problems with divergence could be removed while getting a faster computation time. This will unfortunately not be shown in this text, due to the limitations of the implemented test problems.

Chapter 6

Results for test problems with varying energy

This chapter will look at many of the same elements that was discussed in section 5. Some results are similar, in this case results may not be shown here. This chapter will also try to find out if there is any reason to use SLM instead of KPM on non Hamiltonian systems. The exact solvers does not work when the energy is varying, thus there will be no discussion about that.

6.1 Convergence

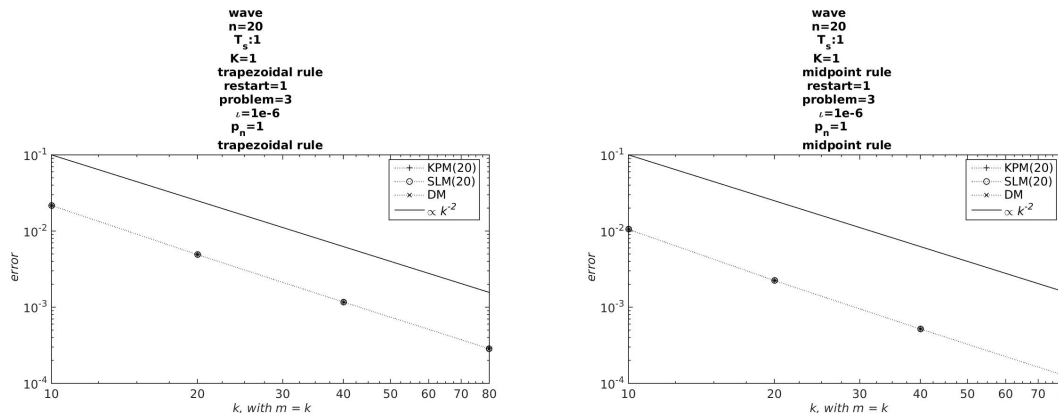
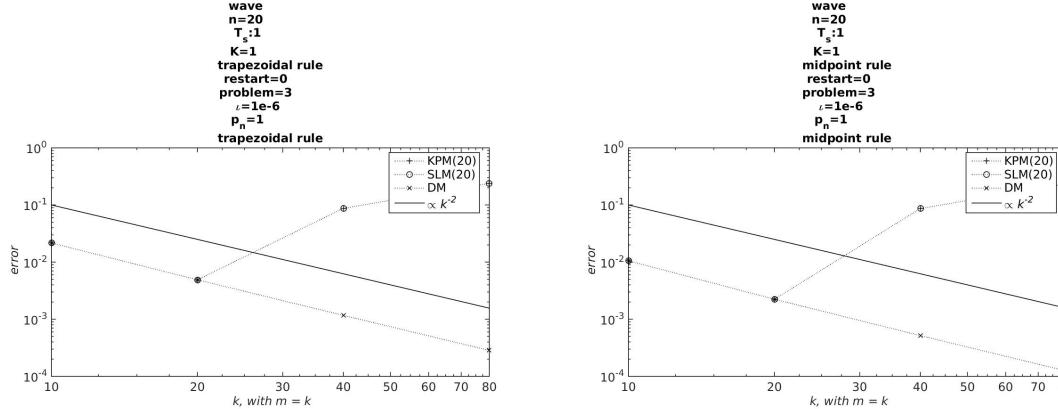


Figure 6.1: Convergence plot with different integrators, and with and without restart simulated over 1 second.

Again midpoint rule performs better than trapezoidal rule. It is interesting to see that without restart the methods does not converge with $n = 20$, while they converged with $n = 2$ when the energy was constant, clearly convergence is a lot harder to achieve in this case.

Only midpoint rule will be used in this chapter.

6.2 Convergence with ι

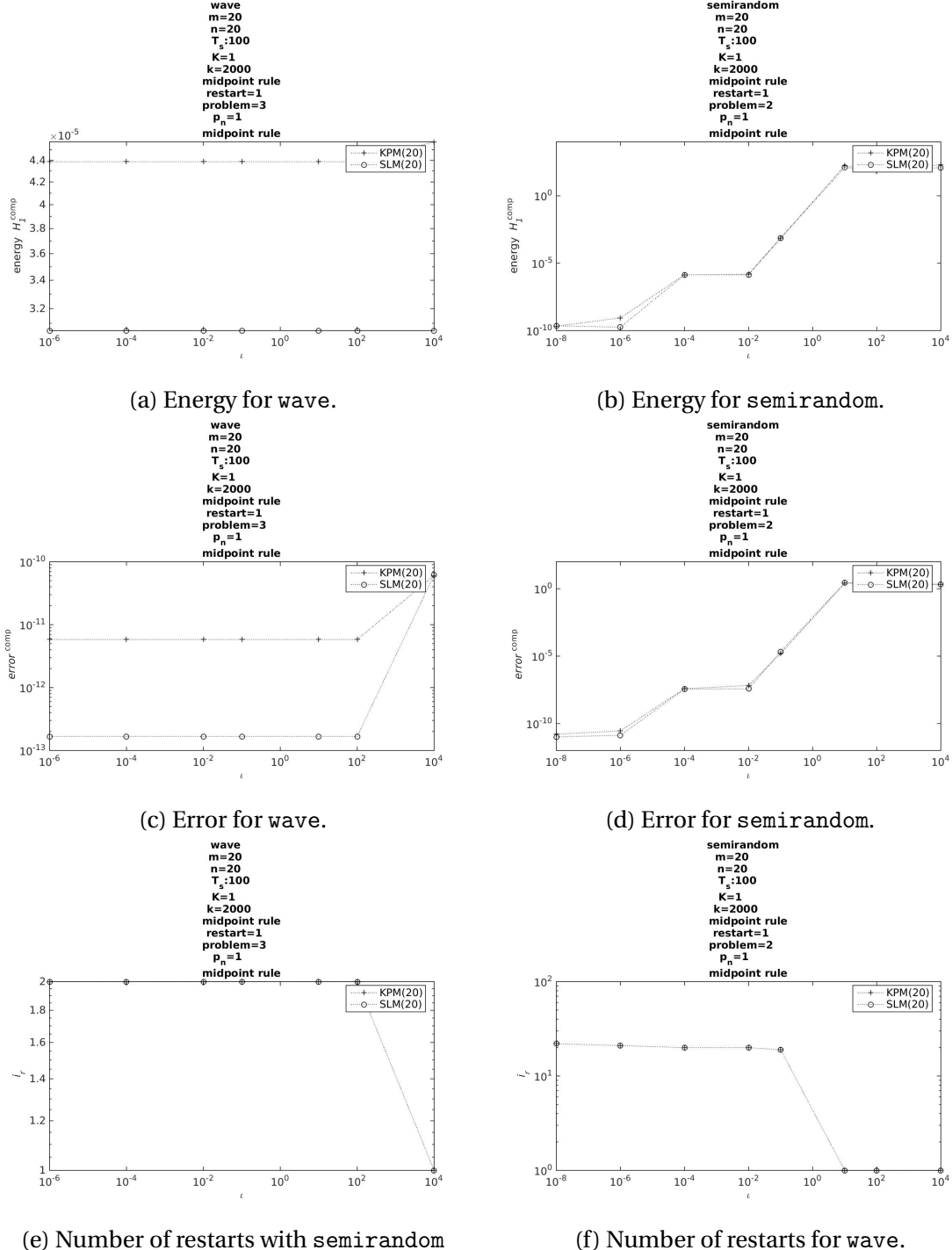


Figure 6.2: These figures show how choosing the correct ι can improve the solution, but also make the program run slower due to excessive restarts. The pictures on the left is for wave and one the right for semirandom. This plot considers 100 seconds, with $n = m = 20$, $k = 2000$, $m = 20$ and midpoint rule.

This look very similar to the one in section 5.4, one important difference is that the energy for SLM no longer starts at $1e - 15$. The difference between SLM and KPM is definitely smaller in this case.

6.3 How to chose n

The pictures in this section look a lot like the pictures in section 5.4, except for the case where restart is used.

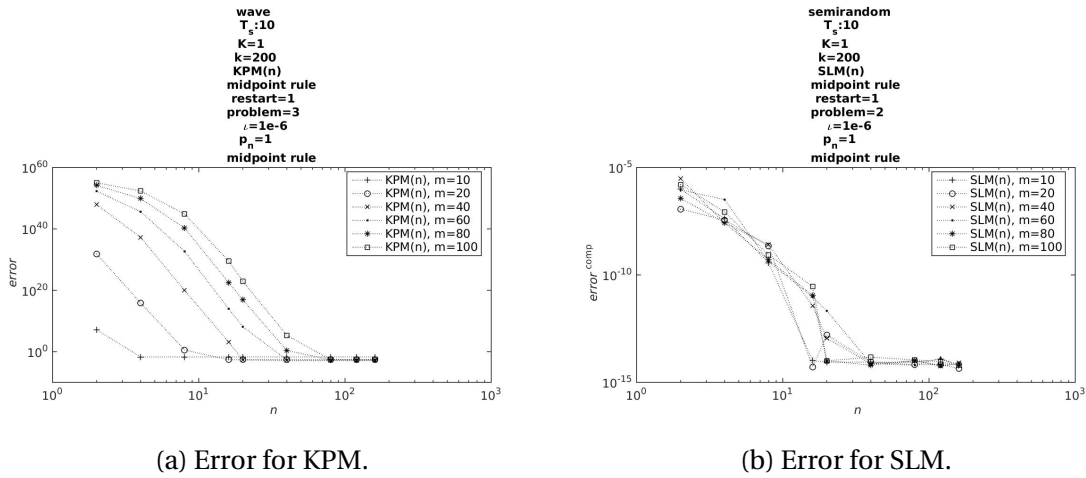


Figure 6.3: The pictures shows which n gives convergence for different m when restart is enabled. This plot is made with midpoint rule with $k = 200$ over 10 seconds.

There is a clear dependance between m and n for KPM. The rule seams to be $n = m$, so that n scales with the square root the size of the matrix, $\hat{m} = 2(m - 2)^2$.

The rule found for KPM seams to work for SLM when m is large enough, even though the difference is not so significant as it is for KPM, larger m tend to need larger n to converge.

6.4 Long time

The pictures that would have been in this section are very similar to the pictures in section 5.5, except for windowing.

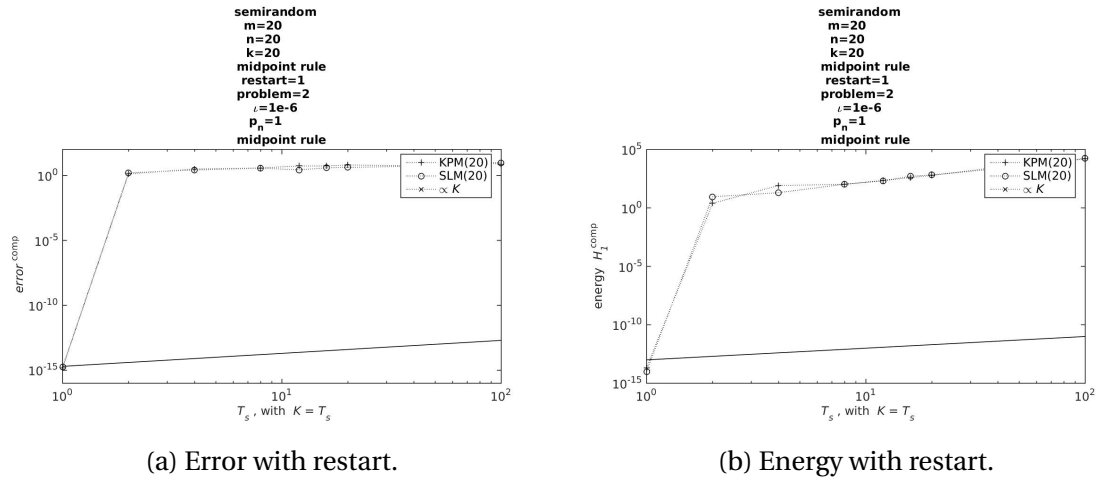


Figure 6.4: Windowing. The restart does not change the result. $m = 20, k = 20$.

Clearly windowing does not work with varying energy, thus the most promising solution strategy from the previous chapter has a very limiting factor.

6.5 Computation time

The run time for varying energy is a little bit different than for the case with constant energy. One of the differences that could be explored is the larger n is needed for larger m , when restart is enabled. This will however not be examined. Instead the computation time under the same assumptions as in 5.8 will be shown as the results are quite different.

6.5.1 Without restart

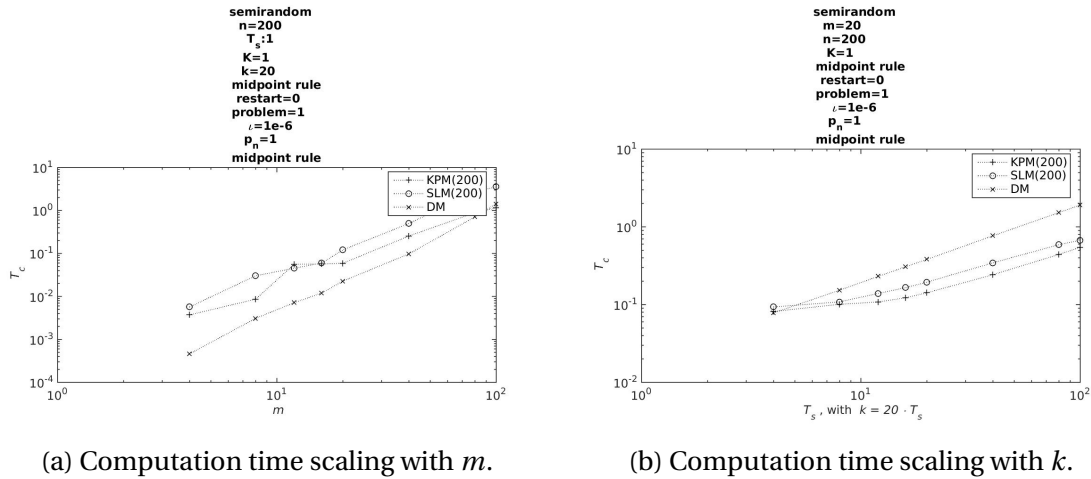


Figure 6.5: A figure of the computation times without restart, $n = 200$, $T_s = 100$, $k = 2000$, and $m = 20$.

The difference between DM and the projection methods are a lot smaller in this case. At the last point DM and KPM are intersecting. KPM becomes faster after this, but SLM does not overtake DM. SLM could be faster than DM if k was large enough.

6.5.2 With restart

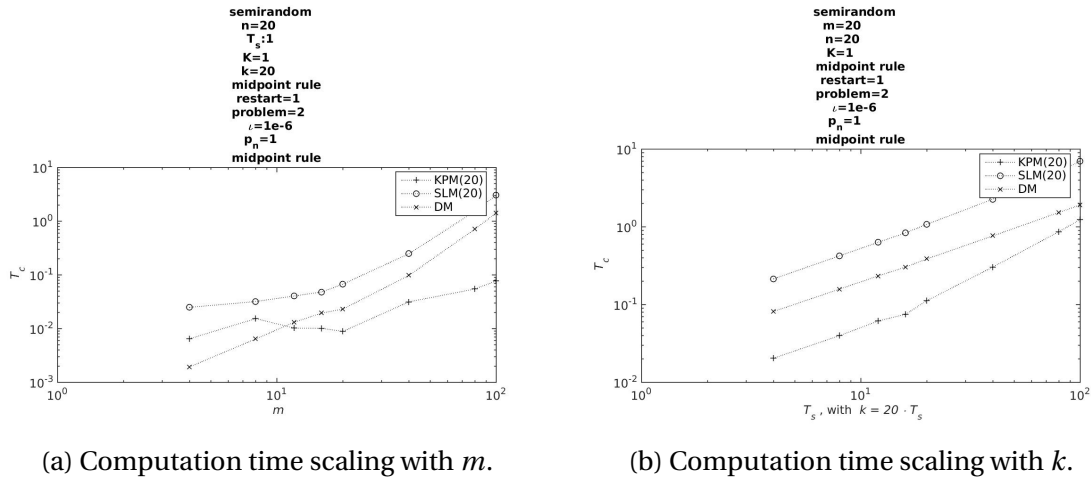


Figure 6.6: A figure of the computation times with restart, $n = 20$, $T_s = 100$, $k = 2000$, and $m = 20$.

Figure 6.6 shows that it can be a good idea to use KPM when m is large and k is small. The faster increase with k for KPM comes from extra number of restarts that KPM needs to ensure

convergence.

It is never wise to use SLM in this case.

Chapter 7

7.1 Code

All code used to create results in the text can be found on github:

<https://github.com/sindreka/Master>

7.2 Further work

The implemented test problems has some limitations. It could be interesting to see how the error and energy behaved with a random Hamiltonian matrix, with a known analytical solution.

Graphics cards are designed to solve 4×4 matrices in parallel [?]. When the energy is constant windowing can be used to ensure convergence with this n . This could then be used to solve non linear Hamiltonian problems in parallel under optimized conditions.

7.3 Conclusion

Use windowing with `expm`, and not `restart`!

Bibliography

- [1] <http://se.mathworks.com/help/matlab/ref/expm.html>.
- [2] Elena Celledoni. <https://www.ntnu.no/ansatte/elenacelledoni>, february 2016.
- [3] C. S. Jog Arup Kumar Nandy. Conservation properties of the trapezoidal rule in linear time domain analysis of acoustics and structures. *FRITA Lab, Department of Mechanical Engineering, Indian Institute of Science, Bangalore, India-560012*, januar 2014.
- [4] Archbishop Richard Bancroft. *King James Bible*. King's Printer Robert Barker, 1604.
- [5] Peter Benner and Heike FaBbender. An Implicitly Restarted SymplecUc Lanczos Method for the Hamlltonlan Eigenvalue Problem. *LINEAR ALGEBRA AND ITS APPLICATIONS* 263:75-111 (1997).
- [6] Peter Benner and Heike FaBbender. An Implicitly Restarted SymplecUc Lanczos Method for the Hamlltonlan Eigenvalue Problem. *LINEAR ALGEBRA AND ITS APPLICATIONS* 263:75-111 (1997).
- [7] M. A. Botchev. A block Krylov subspace time-exact solution method for linear ordinary differential equation systems. *Numer. Linear Algebra Appl.* 2013; 20:557–574, page 557.
- [8] Celledoni E. and Moret I. A Krylov projection method for system of ODEs. *Applied Numerical Mathematics* 23 (1997) 365-378, 1997.
- [9] Celledoni E. and Moret I. A Krylov projection method for system of ODEs. *Applied Numerical Mathematics* 23 (1997) 365-378, page 372, 1997.

- [10] V. Grimm b R.I. McLachlan c D.I. McLaren d D. O’Neale d e B. Owren a G.R.W. Quispel E. Celledoni a. Preserving energy resp. dissipation in numerical PDEs using the “Average Vector Field” method. *Journal of Computational Physics* 231 (2012) 6770–6789, page 6772.
- [11] V. Grimm b R.I. McLachlan c D.I. McLaren d D. O’Neale d e B. Owren a G.R.W. Quispel E. Celledoni a. Preserving energy resp. dissipation in numerical PDEs using the “Average Vector Field” method. *Journal of Computational Physics* 231 (2012) 6770–6789, page 6778.
- [12] Sindre Eskeland. A Krylov projection Method for the heat equation.
- [13] HEIKE FASSBENDER. ERROR ANALYSIS OF THE SYMPLECTIC LANCZOS METHOD FOR THE SYMPLECTIC EIGENVALUE PROBLEM. page 472.
- [14] HEIKE FASSBENDER. ERROR ANALYSIS OF THE SYMPLECTIC LANCZOS METHOD FOR THE SYMPLECTIC EIGENVALUE PROBLEM. *SIAM J. S CI. C OMPUT.* Vol. 35, No. 3, pp. A1376–A1397.
- [15] HEIKE FASSBENDER. ERROR ANALYSIS OF THE SYMPLECTIC LANCZOS METHOD FOR THE SYMPLECTIC EIGENVALUE PROBLEM. *BIT 2000*, Vol. 40, No. 3, pp. 471–496.
- [16] Cohn Henry, Kleinberg Robert, Szegedy Bal azs, and Umans Christopher. Group-theoretic Algorithms for Matrix Multiplication. *Proceedings of the 46th Annual Symposium on Foundations of Computer Science, 23-25 October 2005, Pittsburgh, PA, IEEE Computer Society*, pp. 379-388, 2005.
- [17] Abramowitz Milton and Stegun Irene A. Handbook of Mathematical Functions. Tenth Printing, December 1972. with corrections.
- [18] Heike Faßbender Peter Benner. An Implicitly Restarted SymplecUc Lanczos Method for the Hamlltonian Eigenvalue Problem. *LINEAR ALGEBRA AND ITS APPLICATIONS* 263:75-111, 1997.
- [19] Heike Faßbender Martin Stoll Peter Benner. A Hamiltonian Krylov–Schur-type method based on the symplectic Lanczos process. *Linear Algebra and its Applications*, (435):578–600, 2011.

- [20] Heike Faßbender b Martin Stoll Peter Benner a. A Hamiltonian Krylov–Schur-type method based on the symplectic Lanczos process side 581. *Linear Algebra and its Applications* 435 (2011) 578–600, page 581.
- [21] Heike Faßbender b Martin Stoll Peter Benner a. A Hamiltonian Krylov–Schur-type method based on the symplectic Lanczos process side 581. *Linear Algebra and its Applications* 435 (2011) 578–600.
- [22] Heike Faßbender b Martin Stoll c Peter Benner a. A Hamiltonian Krylov–Schur-type method based on the symplectic Lanczos process. *Linear Algebra and its Applications* 435 (2011) 578–600, page 579.
- [23] Endre Süli and David F. Mayers. *An Introduction to Numerical Analysis*, chapter 7.2 Newton–Cotes formulae, pages 202–203. cambridge university press, 2003.
- [24] Endre Süli and David F. Mayers. *An Introduction to Numerical Analysis*, chapter 12.2 One-step methods, page 317. cambridge university press, 2003.
- [25] Endre Süli and David F. Mayers. *An Introduction to Numerical Analysis*, chapter Definition 10.1, page 286. cambridge university press, 2003.
- [26] David S. Watkins. On Hamiltonian and symplectic Lanczos processes. *Department of Mathematics, Washington State University, Pullman, WA 99164-3113, USA.*
- [27] Saad Yousef. *Iterative Methods for Sparse Linear Systems*, volume SECOND EDITION, chapter 6.3.1, pages 154–155. Siam, 2003. Proposition 6.5.
- [28] Saad Yousef. *Iterative Methods for Sparse Linear Systems*, volume SECOND EDITION, chapter 6.3.1, page 154. Siam, 2003. Algorithm 6.1.